PAUL SCHERRER INSTITUT

Materials Science at Large Scale Facilities

Neutron imaging

Historical

Early neutron imaging (1935–1938)

- Kallmann & Kuhn in Berlin produced the first neutron images using Ra–Be sources and D–D generator.
- First converter–film system and vacuum cassette, similar to later film-based radiography setups.
- Their work was patented in 1940 (*Photographic Detection of Slowly Moving Neutrons*)

First widely recognized neutron radiographs (Peter, 1946)

- Used a high-voltage neutron generator with reduced x-ray background → clearer neutron images.
- Demonstrated two defining neutron imaging strengths:
    - High penetration through dense metals (e.g., faucet).
    - Isotope sensitivity (strong contrast between H_2O and D_2O).

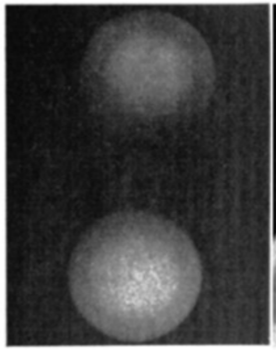

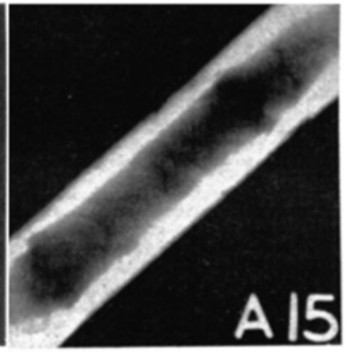

Historical

Reactor era begins (mid-1950s)

- Nuclear reactors (e.g., BEPO) provided orders-of-magnitude higher flux, enabling practical and industrial neutron imaging.
- Technique adopted for non-destructive testing (NDT), especially in nuclear and aerospace sectors.

Field organization and milestones (1960s–1980s)

- First newsletters (1964–1977), first dedicated conference (1973).
- ASTM E545 (1975) → first neutron imaging standard.
- WCNR-1 (1981): major expansion of the community.
- Development of time-resolved imaging and first 3D tomographies (film & TV detectors).

Modern neutron imaging starts (1990s)

Introduction of digital detectors enabled:

- True 3D tomography
- Quantitative image analysis
- High-quality time-resolved imaging

Imaging modalities

Classic neutron imaging methods

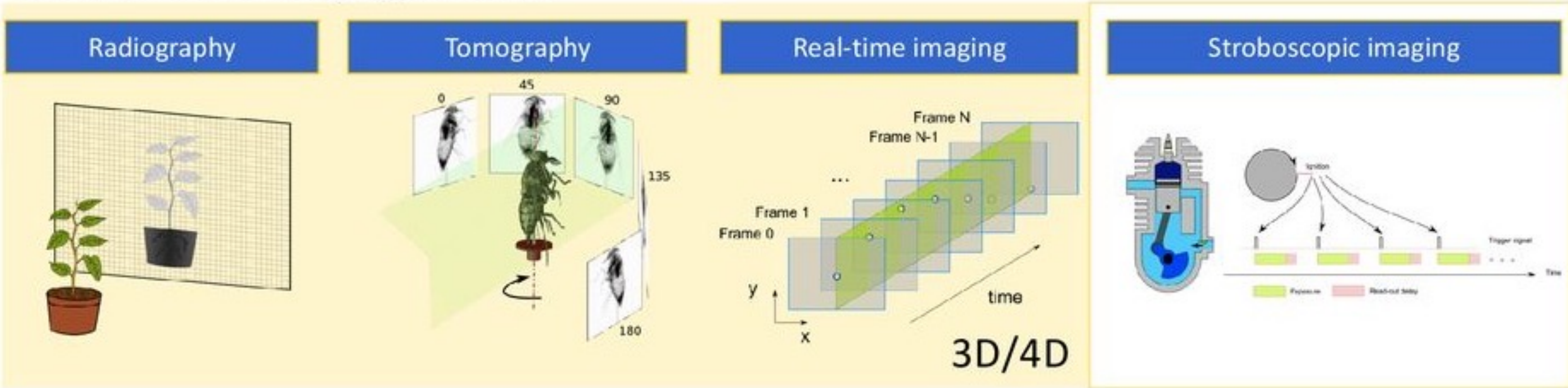

Advanced neutron imaging methods

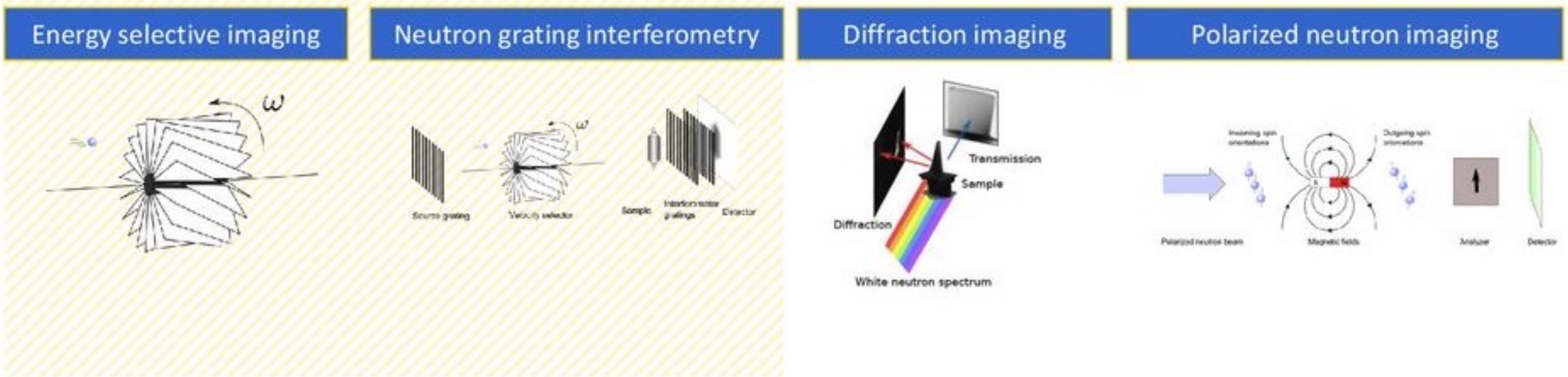

Overview some techniques

Technique	Use When...	Best For	Limitations / Notes
Absorption Contrast Imaging (incl. radiography, tomography)	You want a **direct attenuation-based image** of the sample; you need fast, intuitive visualization; or need 3D structure via tomography.	• Hydrogen-rich materials (water, polymers, oils, adhesives) • Metals that are opaque to X-rays (Al, Ti, Pb) • Multi-material systems (e.g., water in metal)	• Limited by detector efficiency & neutron flux • Spatial resolution typically lower than X-ray imaging • Requires high-quality beam collimation
Neutron Microscope (optical focusing using MLLs or Wolter optics)	You need **micron-scale spatial resolution**, beyond conventional pinhole geometry.	• High-resolution imaging of microstructures in metals or energy materials • Situations requiring both penetration & resolution (e.g., cracks in dense alloys)	• Still developing; lower flux and small field of view • Optics are difficult to fabricate; alignment sensitive
Stroboscopic Neutron Imaging	When you need to study **periodic or cyclic processes** with high temporal precision but low average flux.	• Rotating machinery • Periodic motion in engines, pumps, valves • Repetitive fluid flow or cavitation studies	• Requires strictly periodic motion • Low duty cycle → only suitable for repeatable processes • Synchronization hardware needed

Overview some techniques

Technique	Use When…	Best For	Limitations / Notes
Bragg Edge Imaging	You want to obtain **crystallographic information** in real space — strain, texture, phase distribution — using energy-dependent transmission.	• Mapping strain fields in welded or additively manufactured metals • Distinguishing crystalline phases • Texture gradients in rolled or forged components	• Needs time-of-flight or monochromatic beams • Requires good energy resolution • Interpretation requires modeling (cross-sections, crystallography)
Neutron Grating Interferometry (Talbot–Lau)	You need sensitivity to **microstructure below spatial resolution**, such as micrometer-scale porosity, grain boundaries, or magnetic domain structures (if using polarized neutrons).	• Quantifying microcracks, porosity, voids • Anisotropic microstructure (dark-field contrast) • Fiber orientation in composites • Phase-contrast on soft matter	• Long exposure times • Sensitive to vibrations and sample motion • Modulated intensity limits dynamic imaging
Polarization-Contrast Neutron Imaging	When you want to image **magnetic fields or magnetic microstructure** inside bulk materials, nondestructively.	• Mapping internal magnetic fields in superconductors or permanent magnets • Magnetic domain structures in thick samples • Magnetic shielding quality • Lorentz-force imaging of currents	• Requires polarized beam + spin analyzers • Reduced flux due to polarization optics • Interpretation of magnetic contrast can be non-unique without modeling

Neutron radiography / tomography

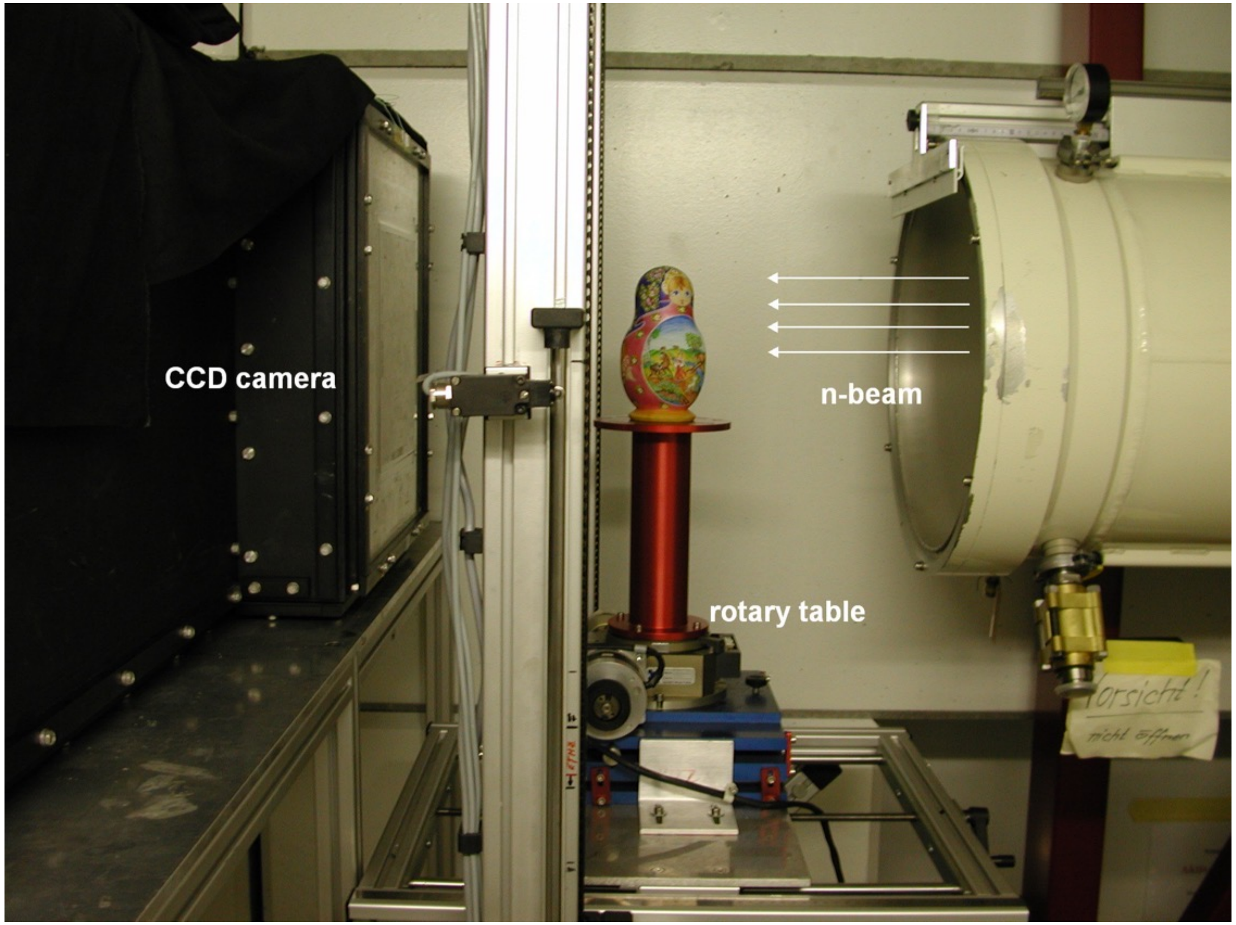

Contrast

Neutron radiography

X-ray radiography

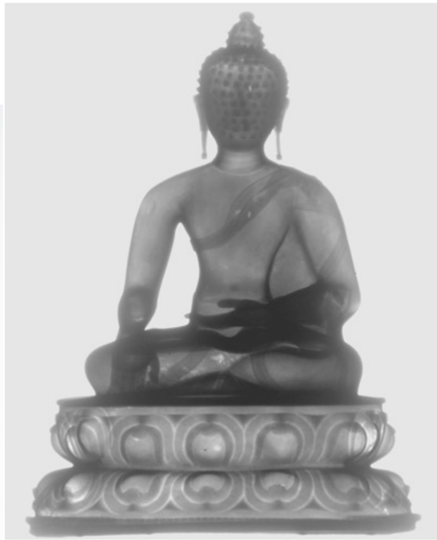

Printed circuit board

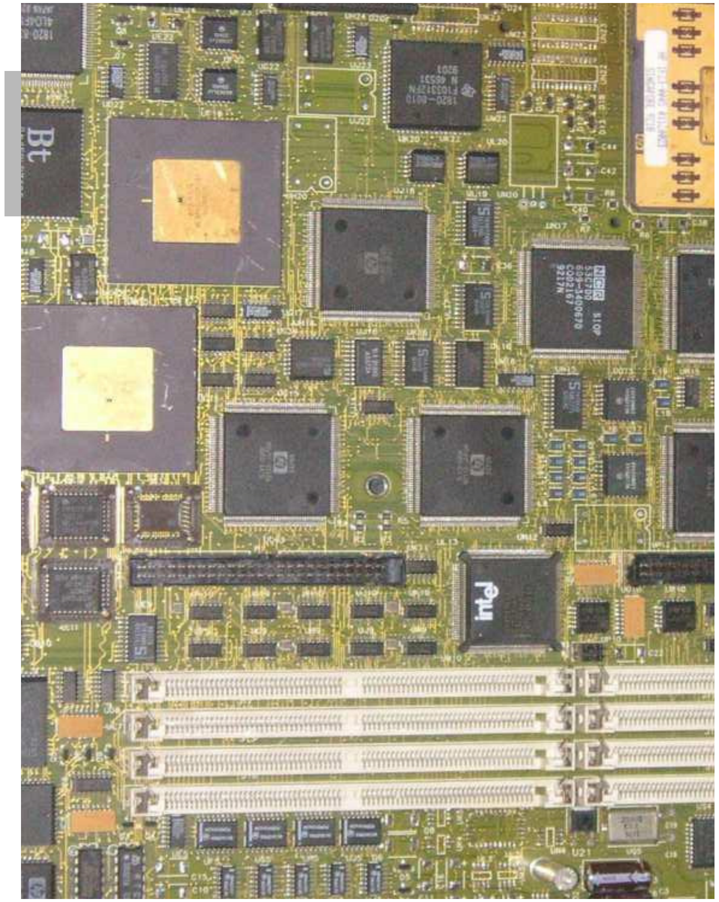

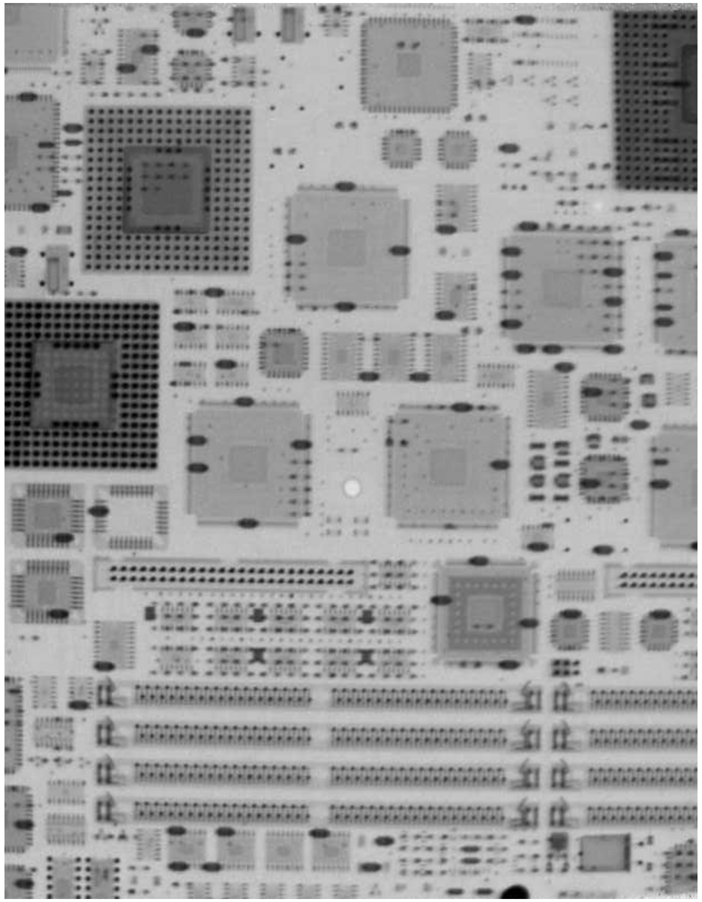

X-ray

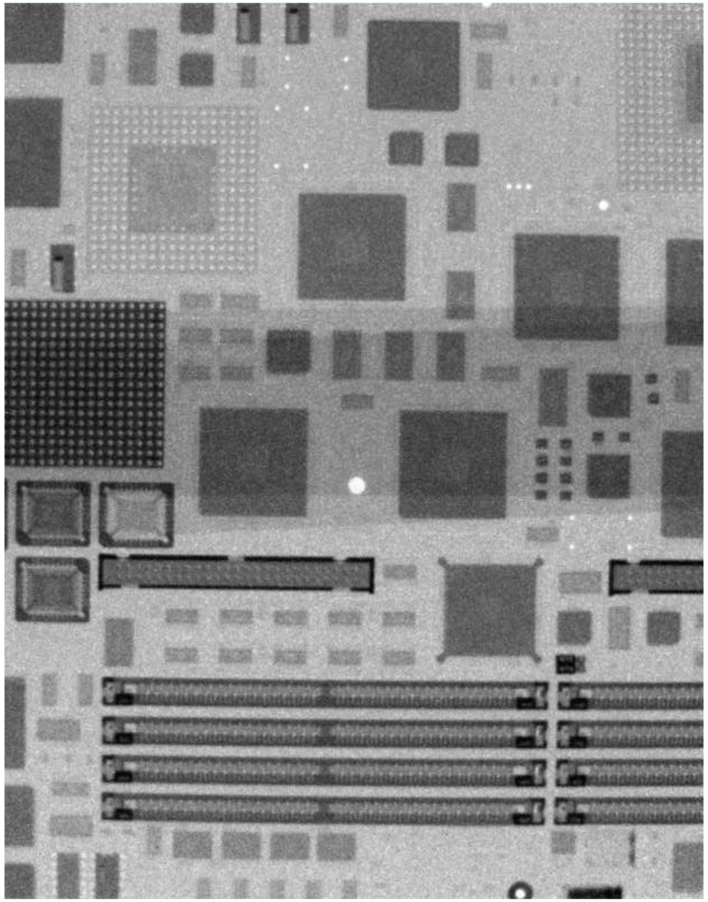

Neutron

Contrast

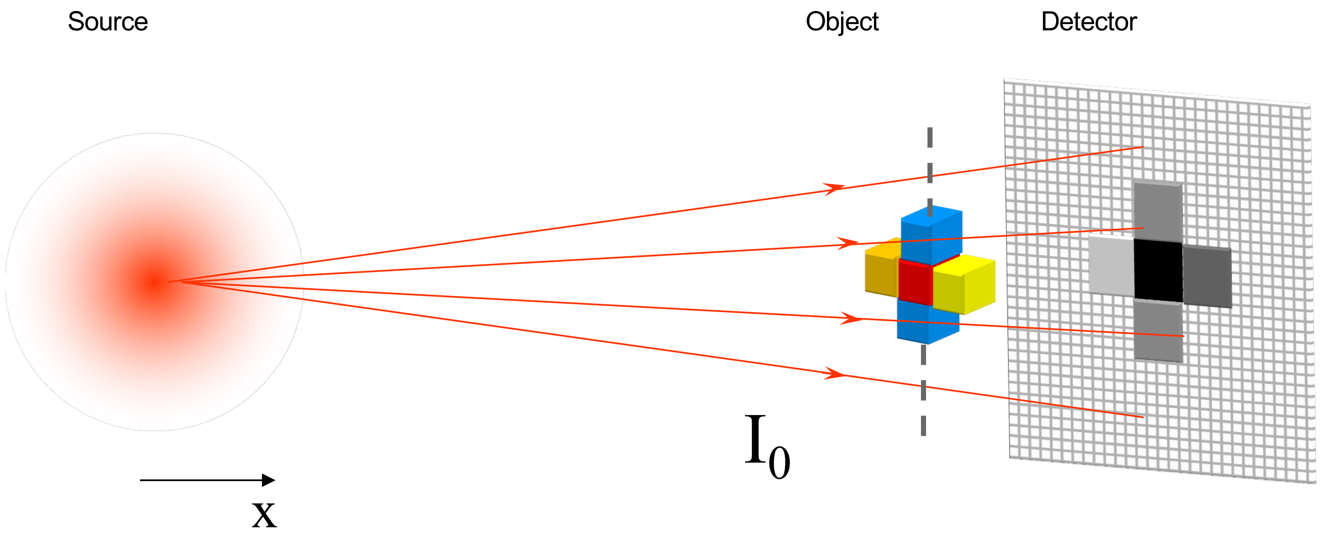

$$I_0 e^{-\int \Sigma(x) dx}$$

I_0 – primary beam

$\Sigma(x)$ – attenuation coefficient

x – propagation direction

Contrast

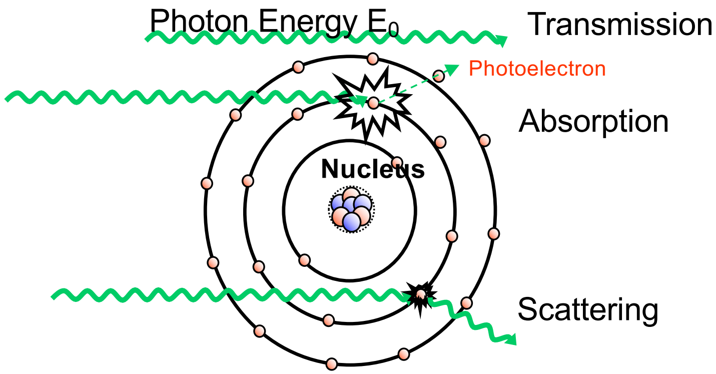

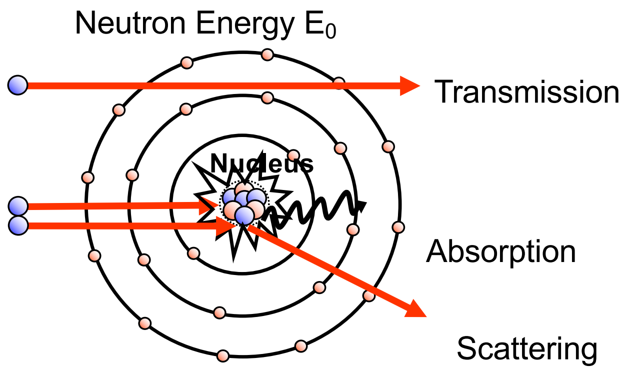

$$I_0 e^{-\int \Sigma(x)dx}$$

$\Sigma = \mathbf{N} \cdot \boldsymbol{\sigma}$

N = number of nuclei per cm^3 .

Unit of Σ is [cm^{-1}]

$\boldsymbol{\sigma} = \boldsymbol{\sigma}_a + \boldsymbol{\sigma}_s$

Unit of σ is [barn] = [10^{-24} cm^2]

X-ray attenuation

Attenuation coefficients with X-ray [cm?^{1}]

1a	2a	3b	4b	5b	6b	7b	8			1b	2b	3a	4a	5a	6a	7a	0
H 0.02																	He 0.02
Li 0.06	Be 0.22											B 0.28	C 0.27	N 0.11	O 0.16	F 0.14	Ne 0.17
Na 0.13	Mg 0.24											Al 0.38	Si 0.33	P 0.25	S 0.30	Cl 0.23	Ar 0.20
K 0.14	Ca 0.26	Sc 0.48	Ti 0.73	V 1.04	Cr 1.29	Mn 1.32	Fe 1.57	Co 1.78	Ni 1.96	Cu 1.97	Zn 1.64	Ga 1.42	Ge 1.33	As 1.50	Se 1.23	Br 0.90	Kr 0.73
Rb 0.47	Sr 0.86	Y 1.61	Zr 2.47	Nb 3.43	Mo 4.29	Tc 5.06	Ru 5.71	Rh 6.08	Pd 6.13	Ag 5.67	Cd 4.84	In 4.31	Sn 3.98	Sb 4.28	Te 4.06	I 3.45	Xe 2.53
Cs 1.42	Ba 2.73	La 5.04	Hf 19.70	Ta 25.47	W 30.49	Re 34.47	Os 37.92	Ir 39.01	Pt 38.61	Au 35.94	Hg 25.88	Tl 23.23	Pb 22.81	Bi 20.28	Po 20.22	At	Rn 9.77
Fr	Ra 11.80	Ac 24.47	Rf	Ha													
Lanthanides	Ce 5.79	Pr 6.23	Nd 6.46	Pm 7.33	Sm 7.68	Eu 5.66	Gd 8.69	Tb 9.46	Dy 10.17	Ho 10.91	Er 11.70	Tm 12.49	Yb 9.32	Lu 14.07			
*Actinides	Th 28.95	Pa 39.65	U 49.08	Np	Pu	Am	Cm	Bk	Vf	Es	Fm	Md	No	Lr x-ray			

Neutron attenuation

Attenuation coefficients with neutrons [cm?^{1}]

1a	2a	3b	4b	5b	6b	7b	8			1b	2b	3a	4a	5a	6a	7a	0
H 3.44																	He 0.02
Li 3.30	Be 0.79											B 101.60	C 0.56	N 0.43	O 0.17	F 0.20	Ne 0.10
Na 0.09	Mg 0.15											Al 0.10	Si 0.11	P 0.12	S 0.06	Cl 1.33	Ar 0.03
K 0.06	Ca 0.08	Sc 2.00	Ti 0.60	V 0.72	Cr 0.54	Mn 1.21	Fe 1.19	Co 3.92	Ni 2.05	Cu 1.07	Zn 0.35	Ga 0.49	Ge 0.47	As 0.67	Se 0.73	Br 0.24	Kr 0.61
Rb 0.08	Sr 0.14	Y 0.27	Zr 0.29	Nb 0.40	Mo 0.52	Tc 1.76	Ru 0.58	Rh 10.88	Pd 0.78	Ag 4.04	Cd 115.11	In 7.58	Sn 0.21	Sb 0.30	Te 0.25	I 0.23	Xe 0.43
Cs 0.29	Ba 0.07	La 0.52	Hf 4.99	Ta 1.49	W 1.47	Re 6.85	Os 2.24	Ir 30.46	Pt 1.46	Au 6.23	Hg 16.21	Tl 0.47	Pb 0.38	Bi 0.27	Po	At	Rn
Fr	Ra 0.34	Ac	Rf	Ha													
*Lanthanides	Ce 0.14	Pr 0.41	Nd 1.87	Pm 5.72	Sm 171.47	Eu 94.58	Gd 1479.04	Tb 0.93	Dy 32.42	Ho 2.25	Er 5.48	Tm 3.53	Yb 1.40	Lu 2.75			
**Actinides	Th 0.59	Pa 8.46	U 0.82	Np 9.80	Pu 50.20	Am 2.86	Cm	Bk	Cf	Es	Fm	Md	No	Lr neut.			

Water uptake in plants

- D_2O as contrast agent

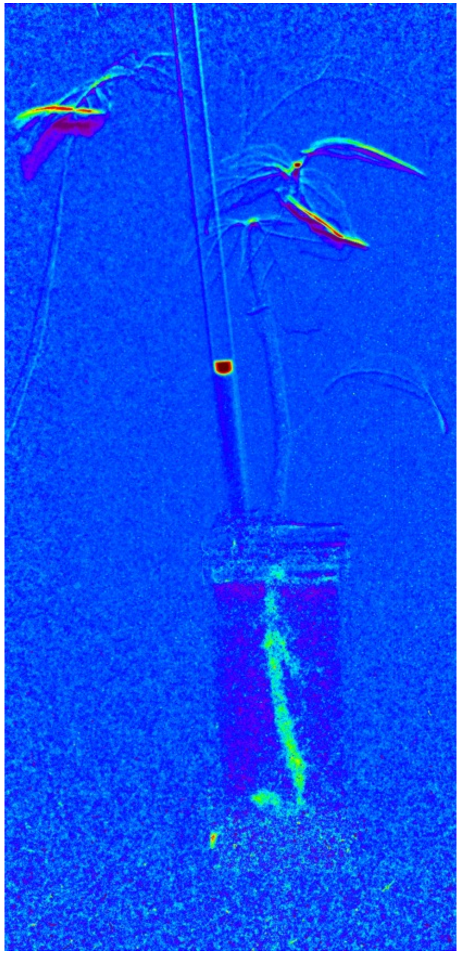

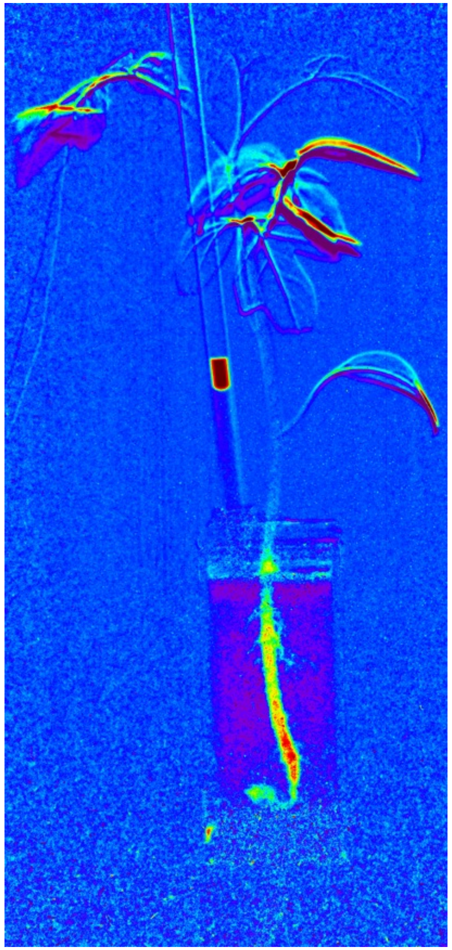

Water uptake in plants in 3D

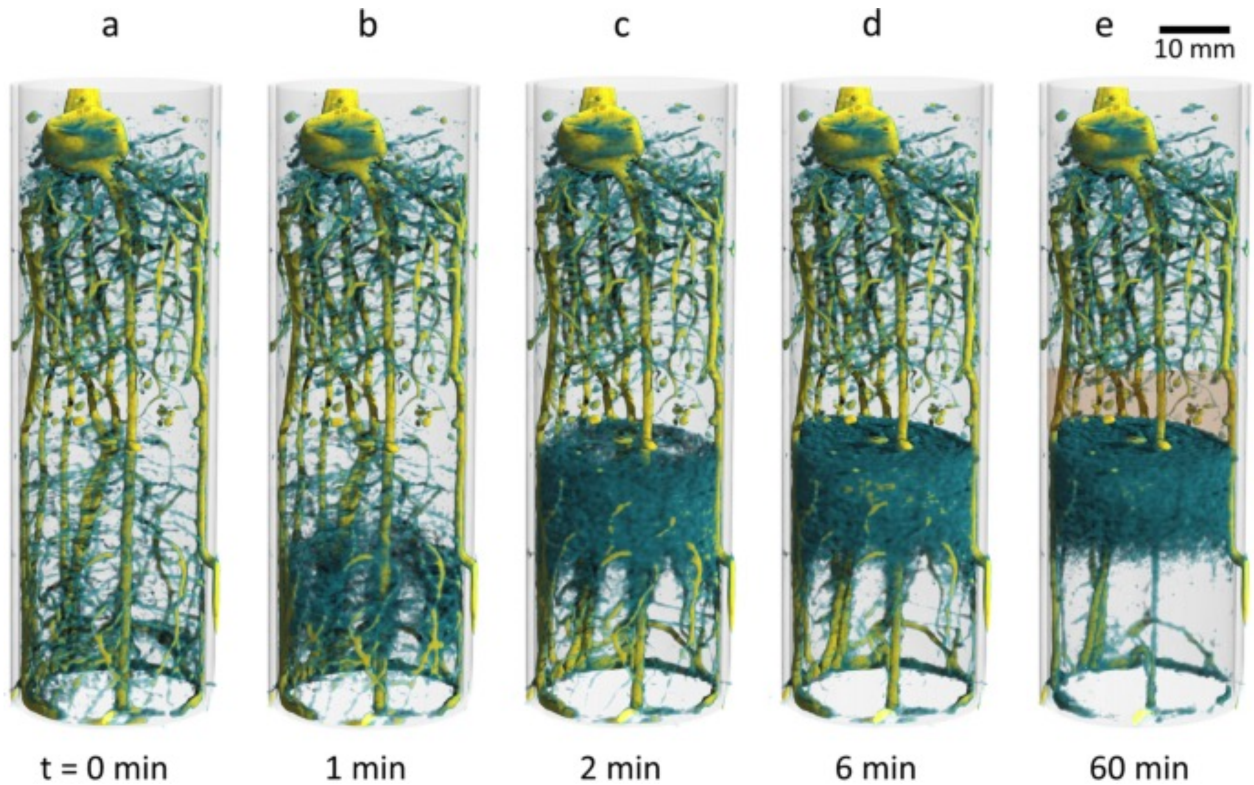

Time-resolved neutron tomography of a 13-days-old maize root system after infiltration of 4 ml deuterated water

C. Töztke et al. Scientific Reports **11,**, 0578 (2021)

Combining X-ray and neutron imaging

Cross-sections

Total neutron cross section

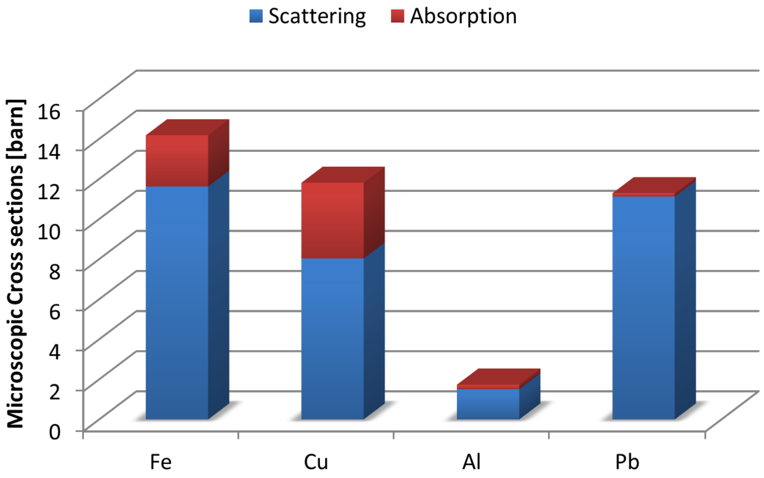

$$\sigma = \sigma_a + \sigma_s$$

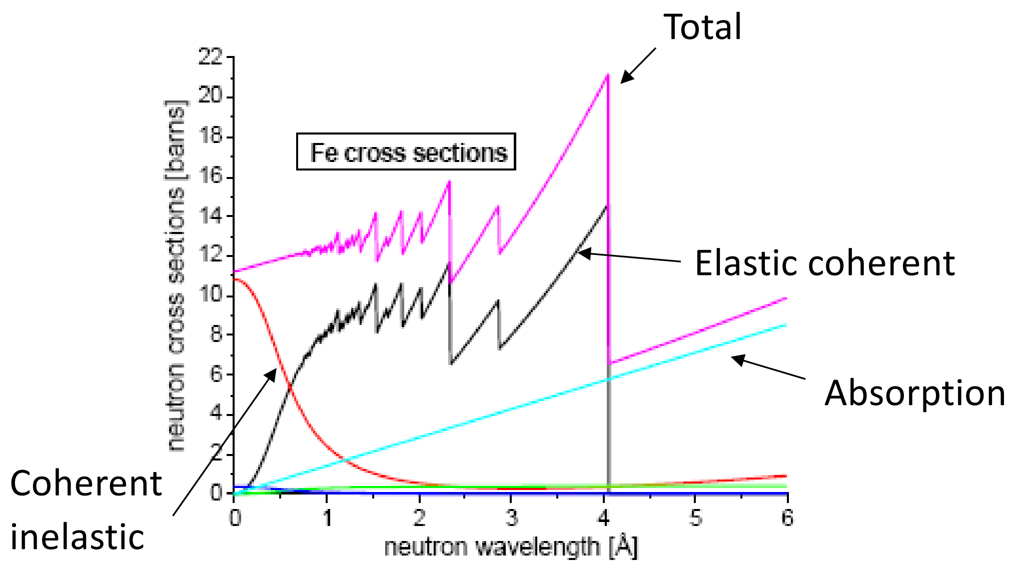

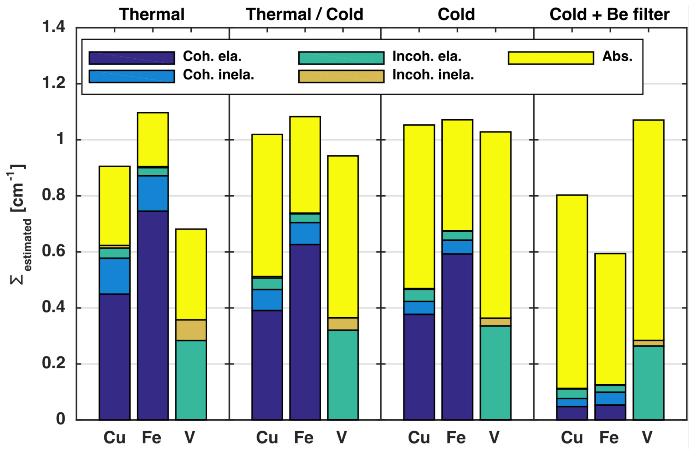

Resolution

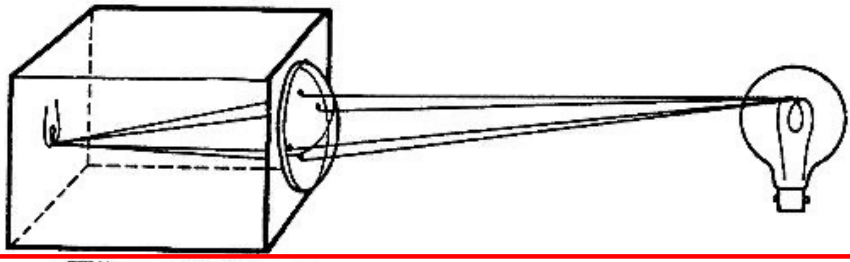

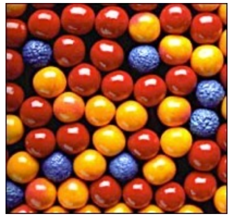

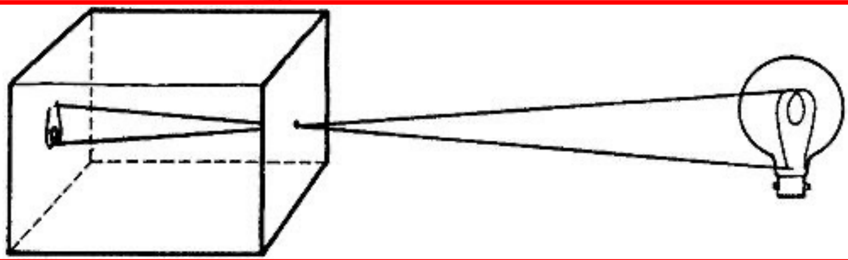

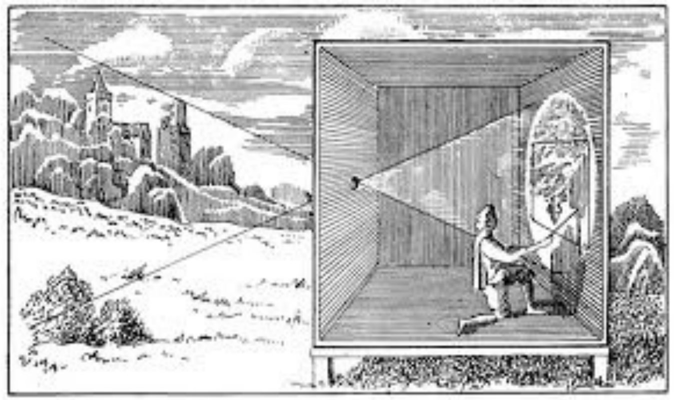

Simplified setup

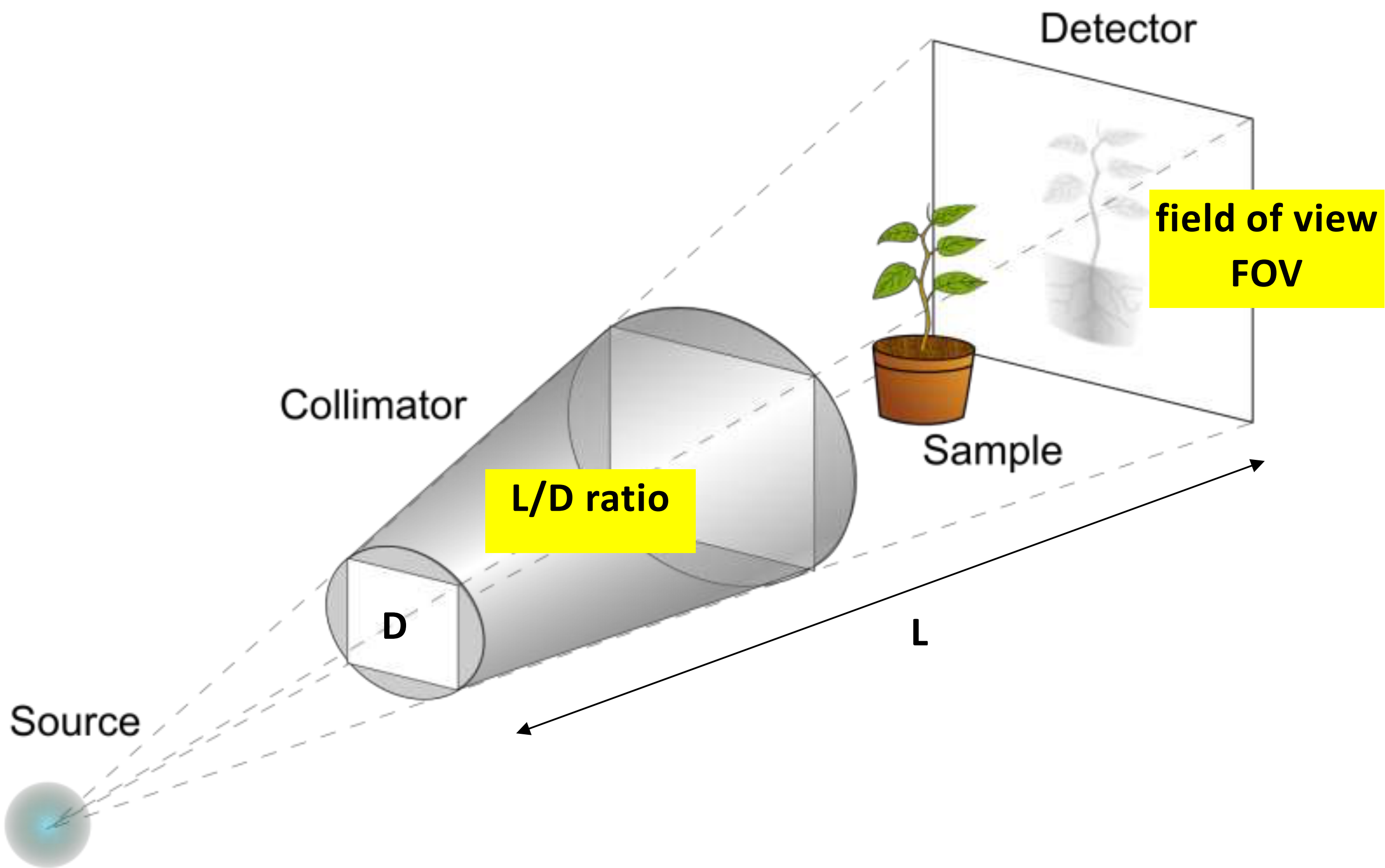

Influence geometry

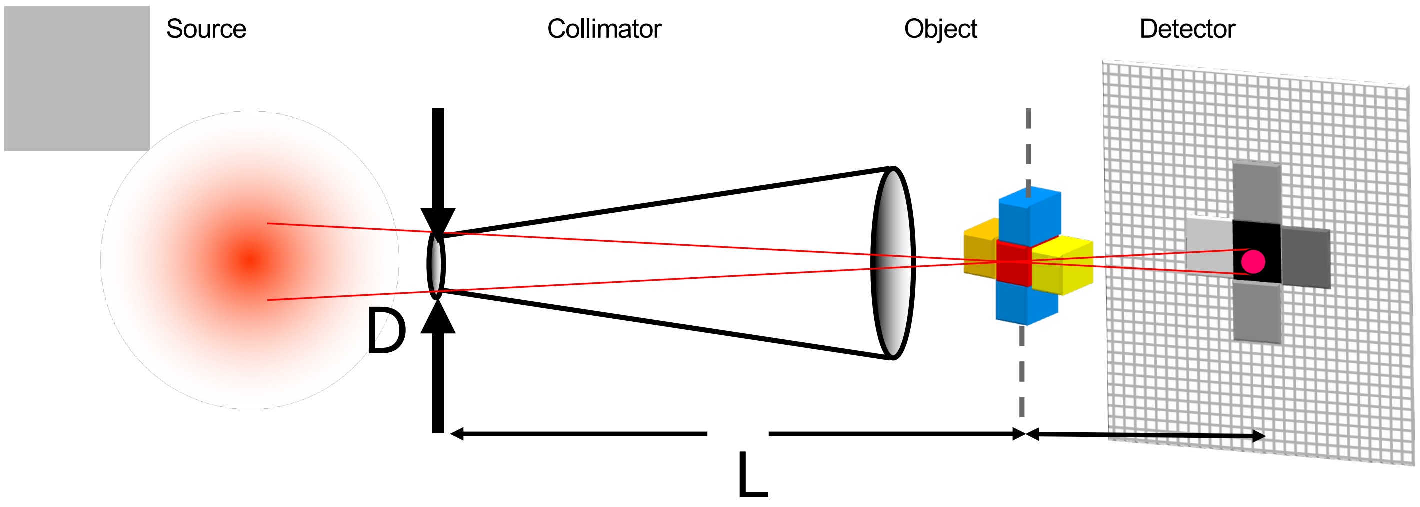

collimation ratio L/D typical: several 100

Influence geometry

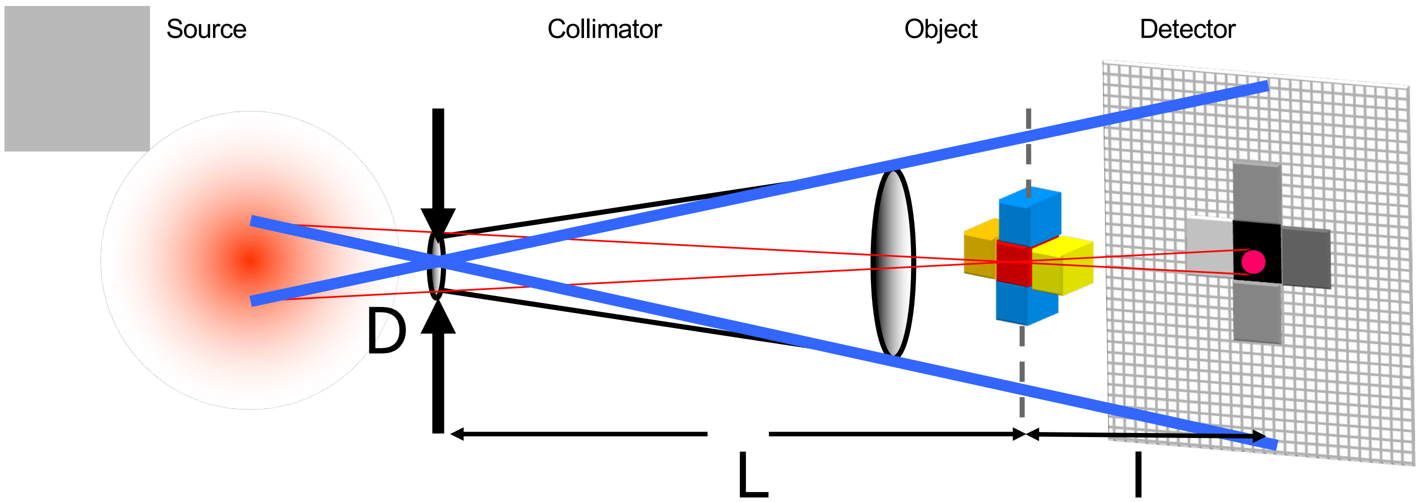

$$\text{blur } d = \frac{l}{L/D}$$

Influence geometry

flux limitations $10^9\ cm^{-2}s^{-1}$

blur $d = \frac{l}{L/D}$

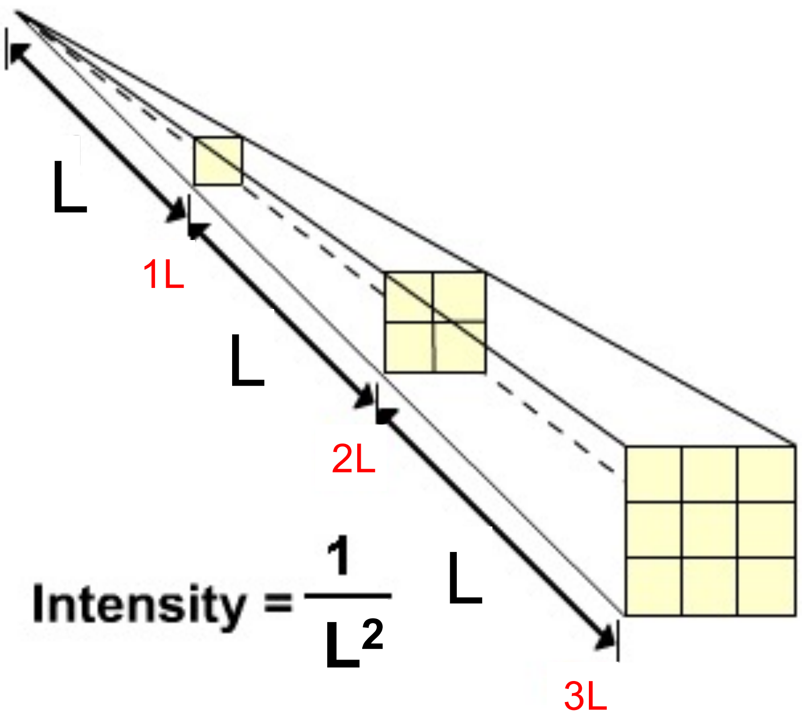

$$\text{Intensity} = \frac{1}{L^2}$$

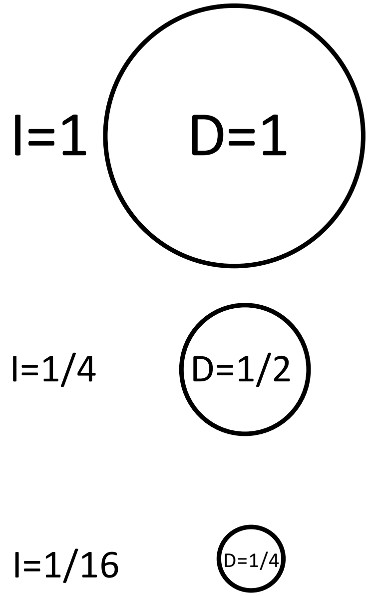

Intensity = D²

Influence geometry

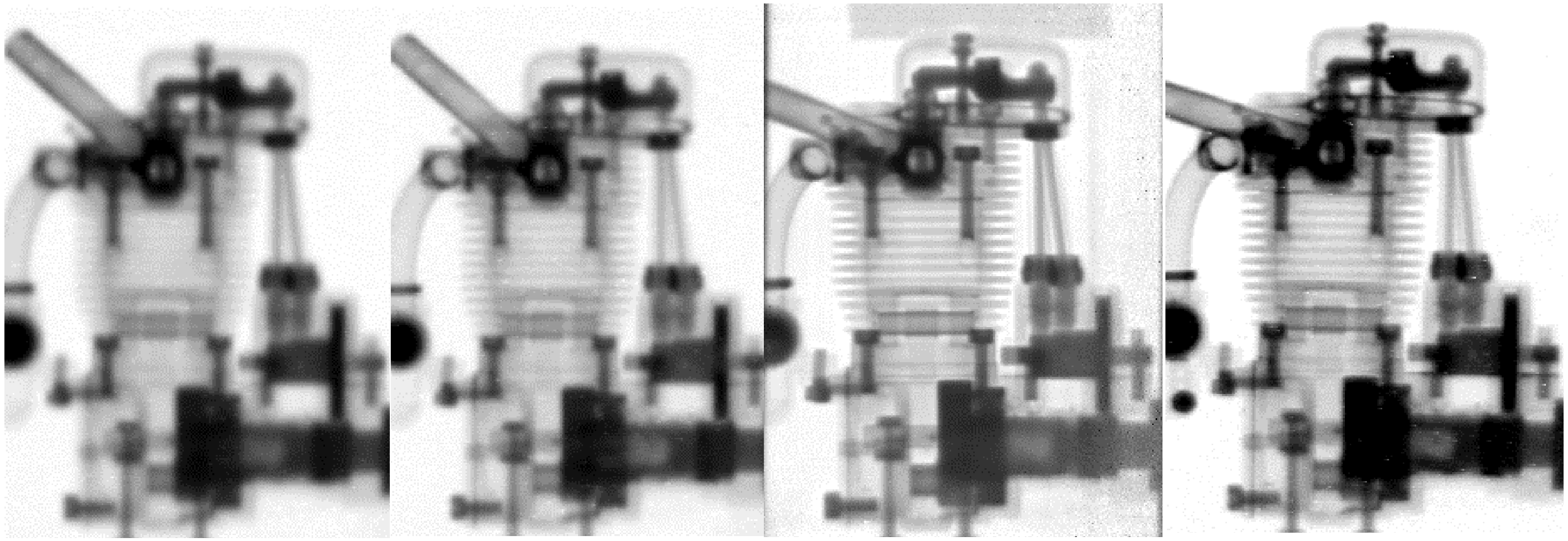

L/D=71 L/D=115 L/D=320 L/D>500.

Radiographs of a small motor taken at different beam positions with different L/D ratios.

Courtesy B. Schillinger, TUM

Time resolved neutron radiography

Fast neutron imaging

- Neutron flux is relatively low as compared to sychrotrons x-ray flux. Difficult to perform fast in situ measurements.
- Except for periodical processes, here one can work in stroboscopic mode
- Advantage:
  - the number of neutrons/photons in one time window is still very low, but many exposures of the same time window of the periodic process may be accumulated on the detector before read-out, thus increasing the available intensity
- Disadvantage:
  - Only one time window of the periodic process can be recorded in one sequence, the periodic process has to be recorded in a sequence of many consecutive time window accumulations, sacrificing most neutrons.

Radiography / tomography stroboscopic mode

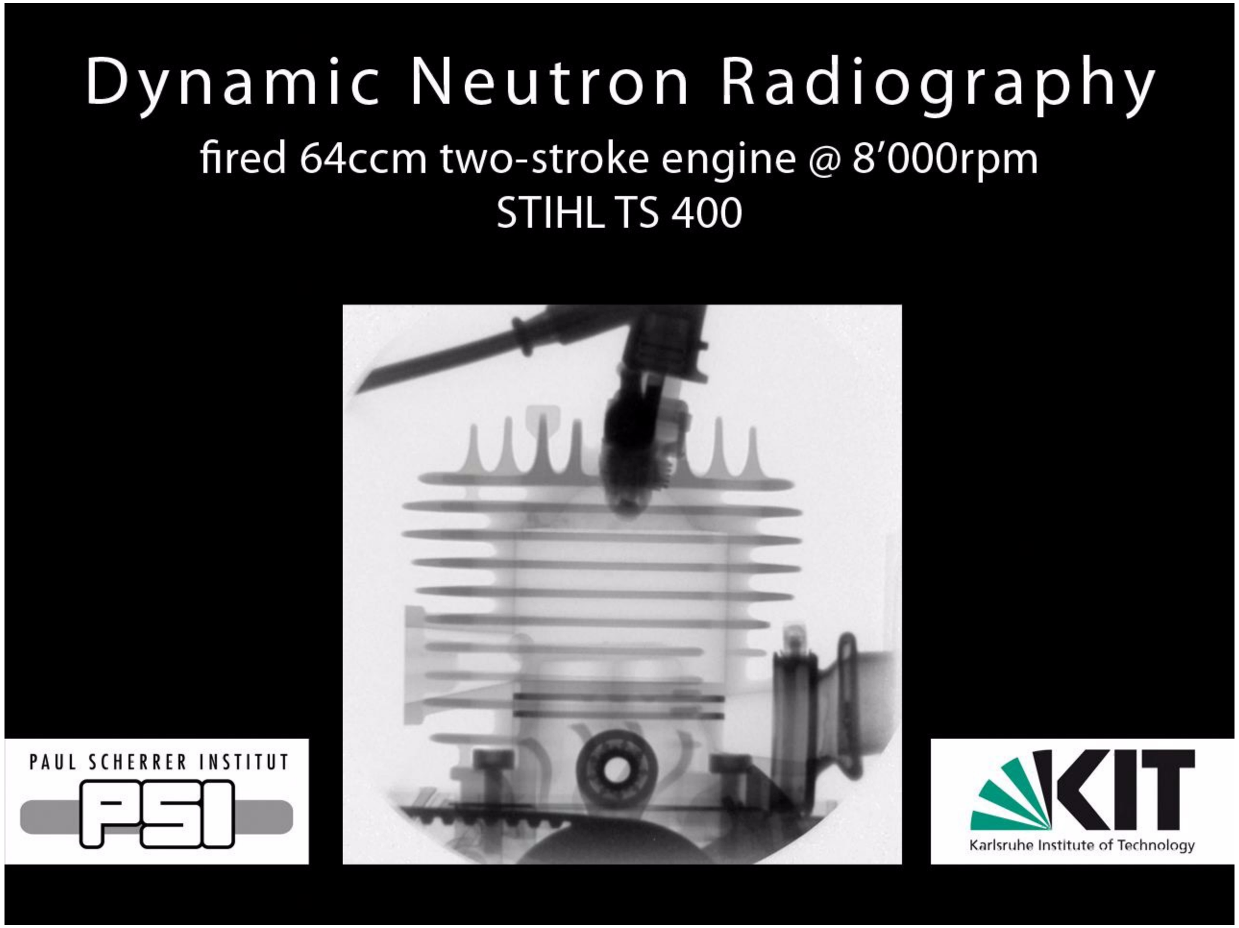

Neutron microscope

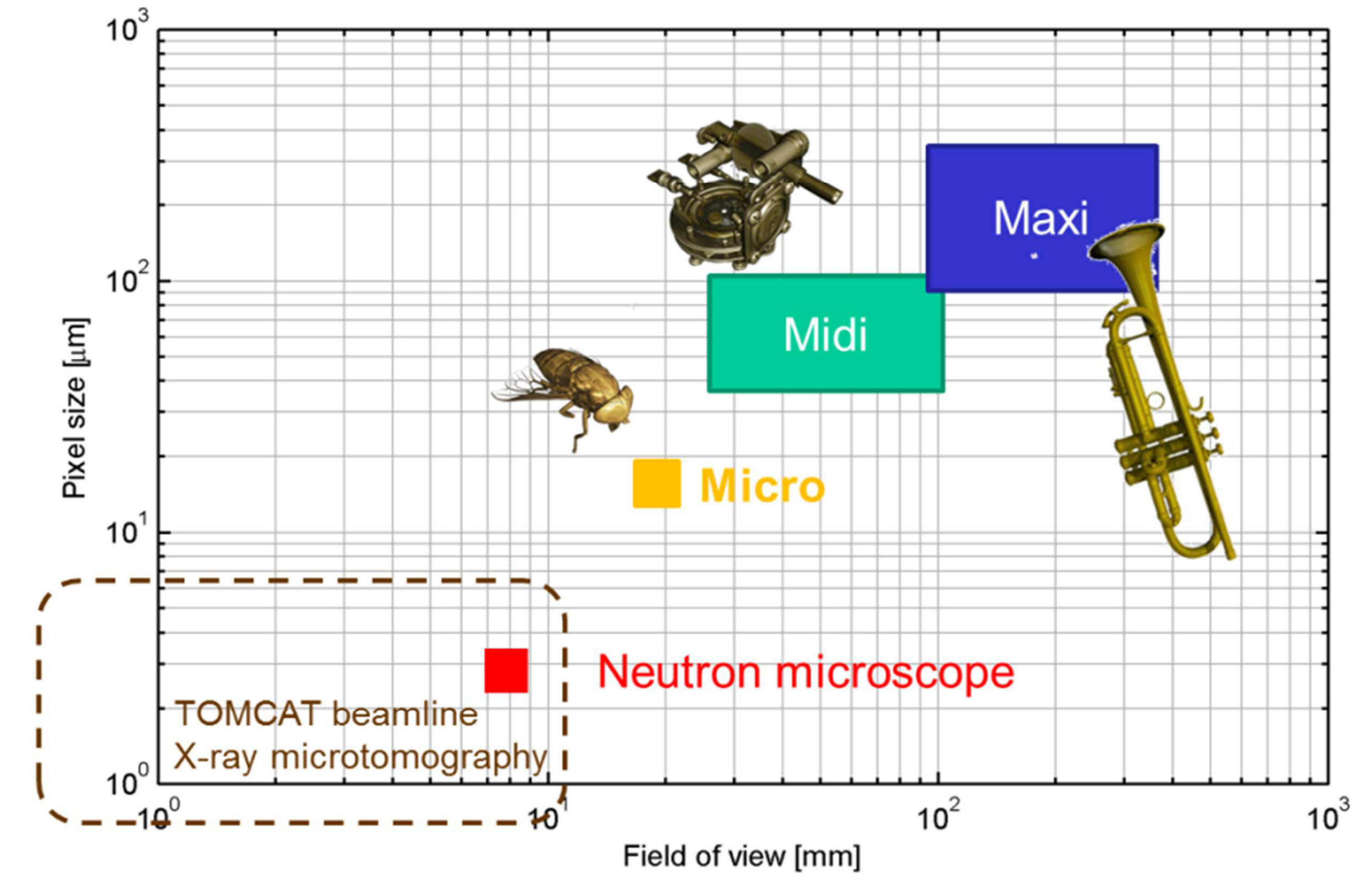

Neutron microscope

The dedicated objective is designed for a field of view of 10 mm x 10 mm and the object distance is 60 mm. It is composed of thirteen individual lenses. The scintillator screen is based an isotopically-enriched 157-gadolinium oxysulfide.

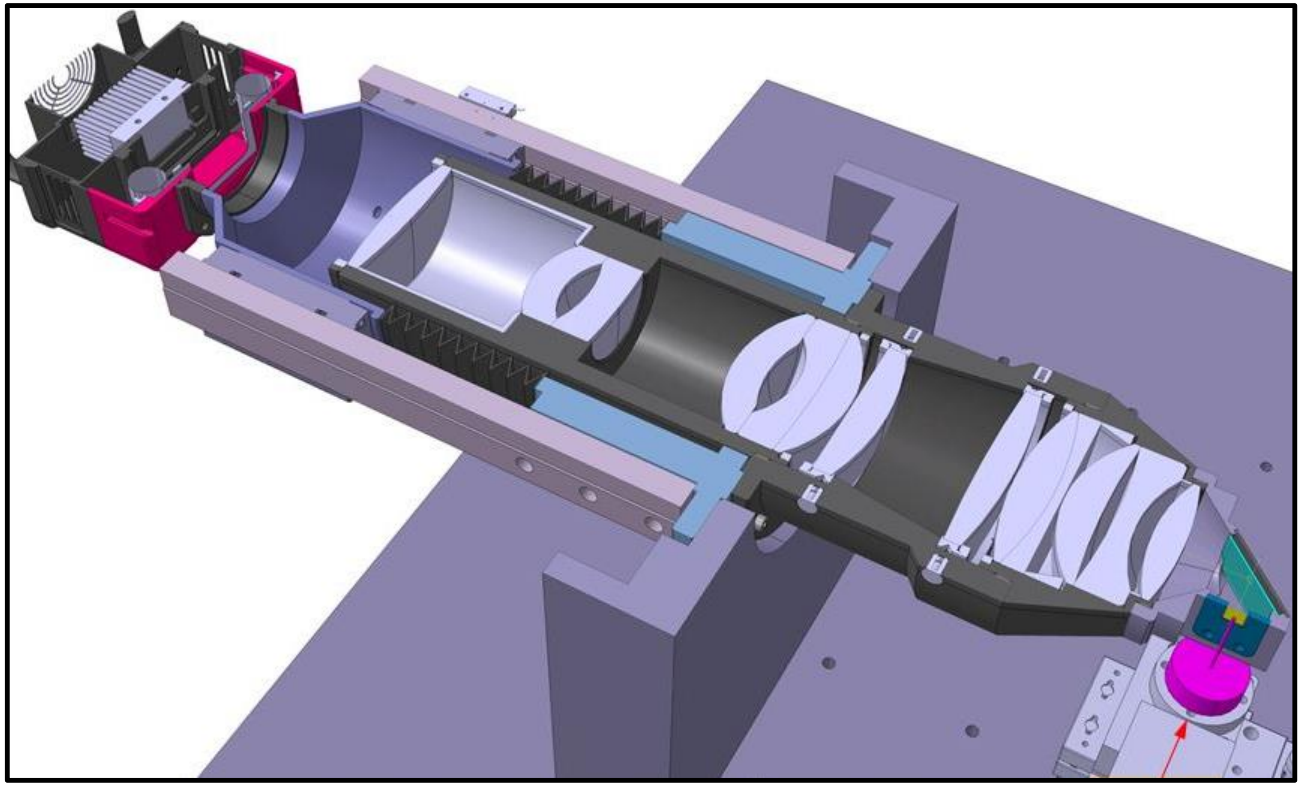

Neutron microscope

- Siemens star
- Resolution = 5.4µm

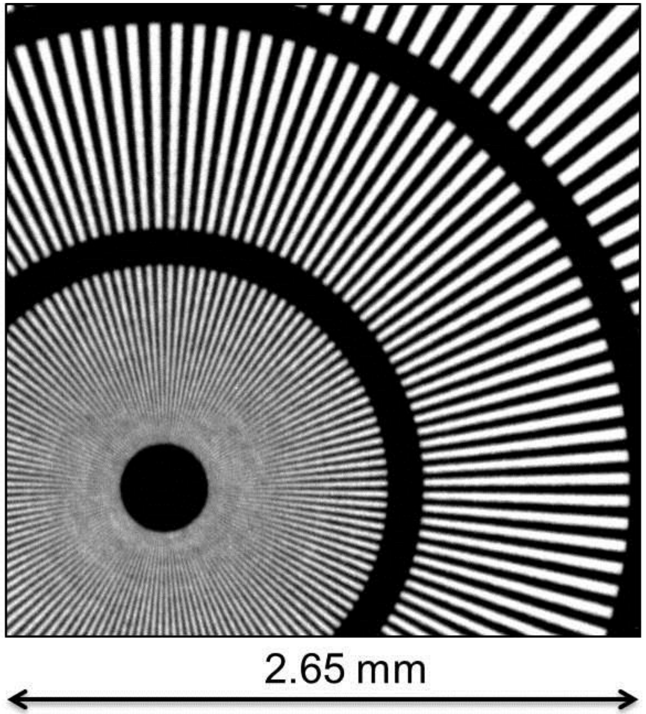

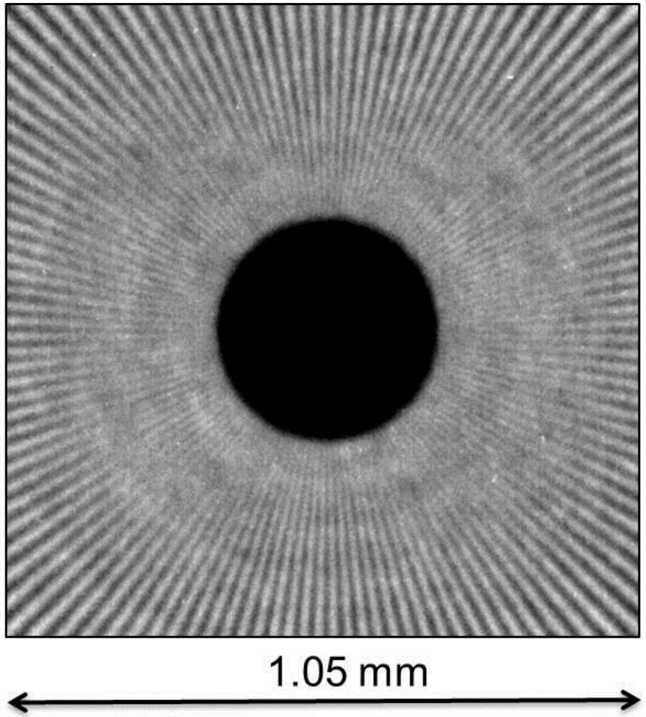

Beyond attenuation contrast

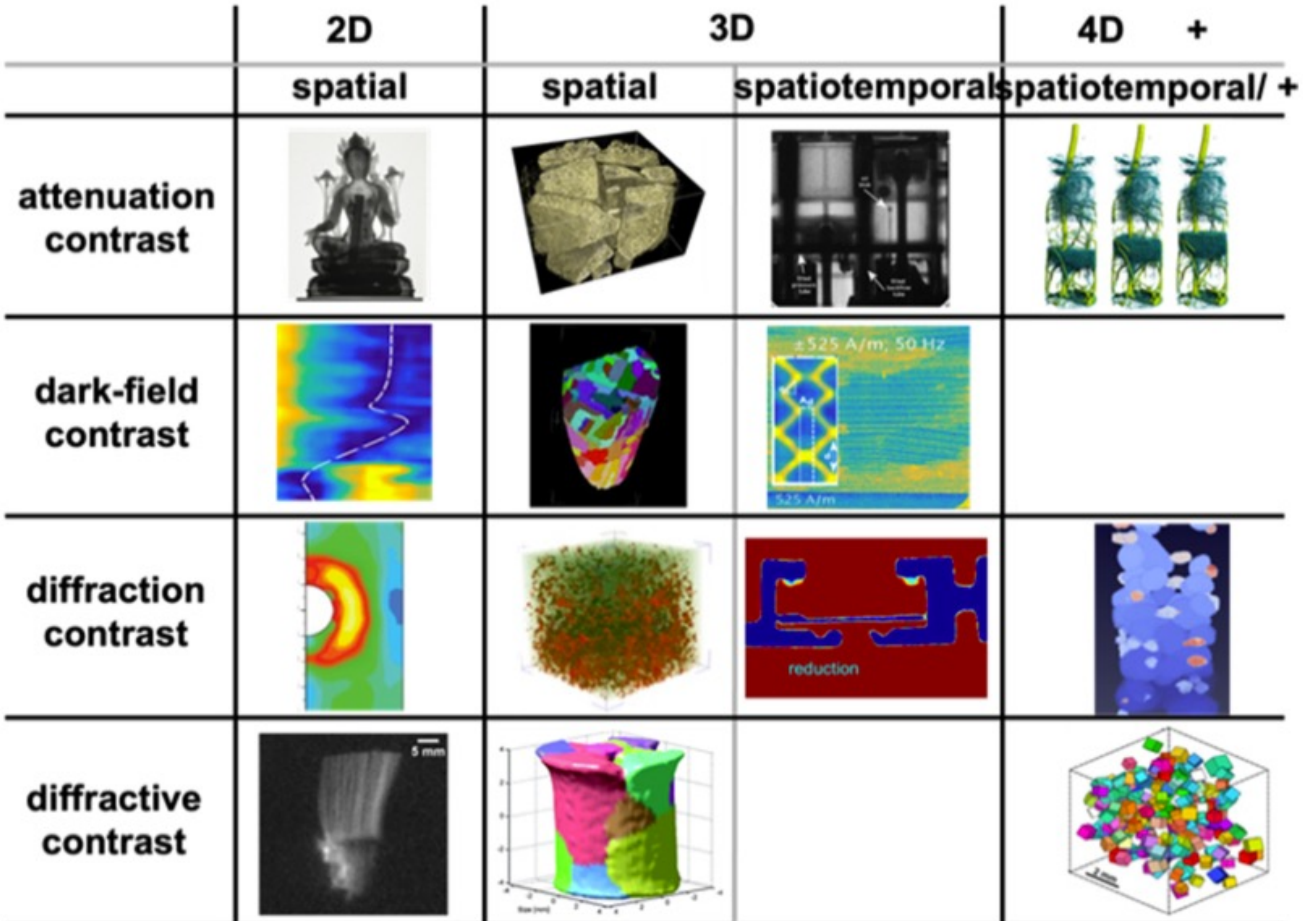

Beyond attenuation contrast

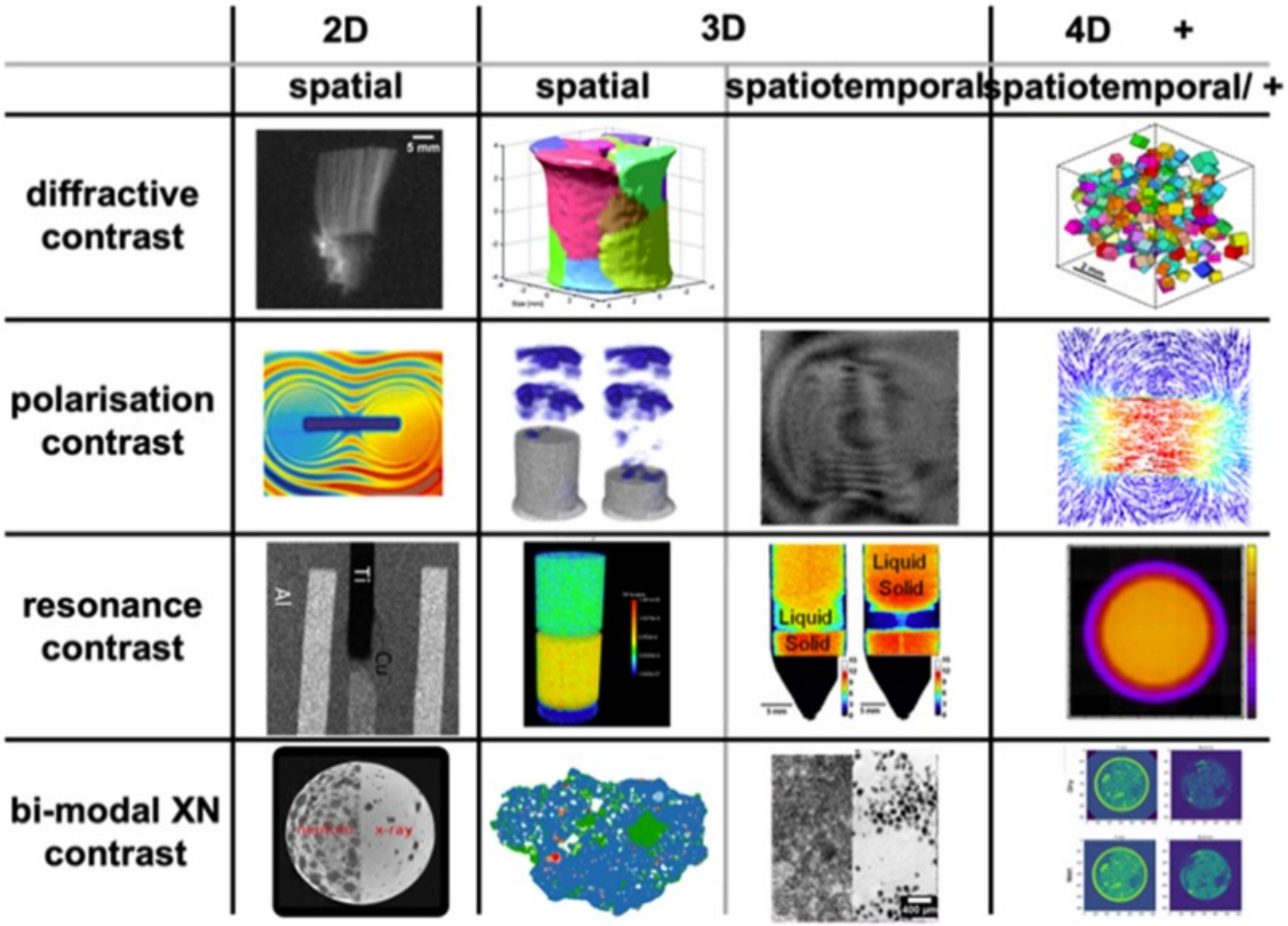

Imaging modalities

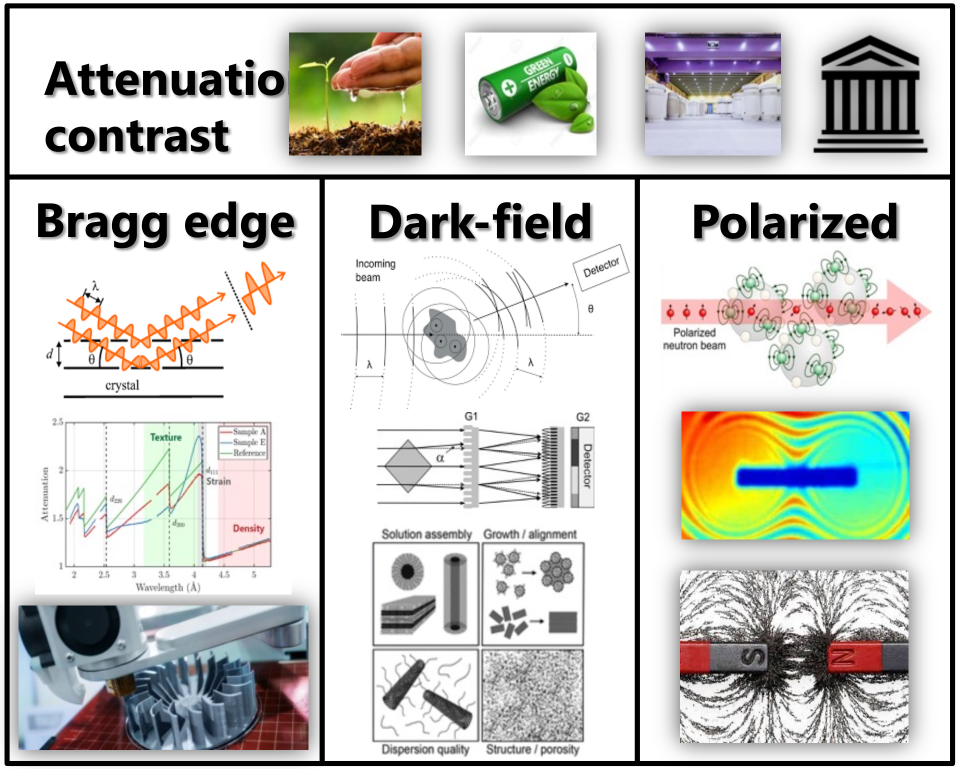

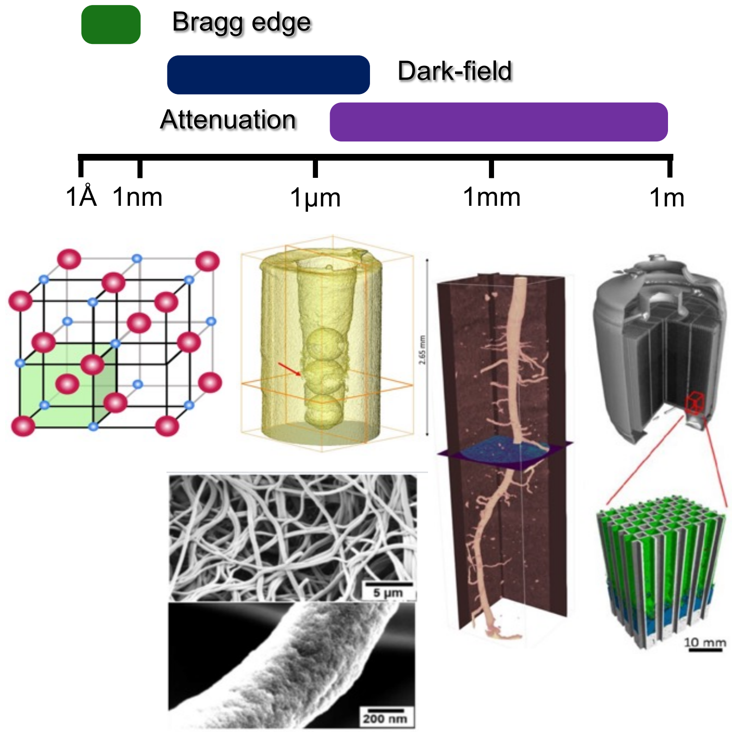

Neutron Bragg edge imaging

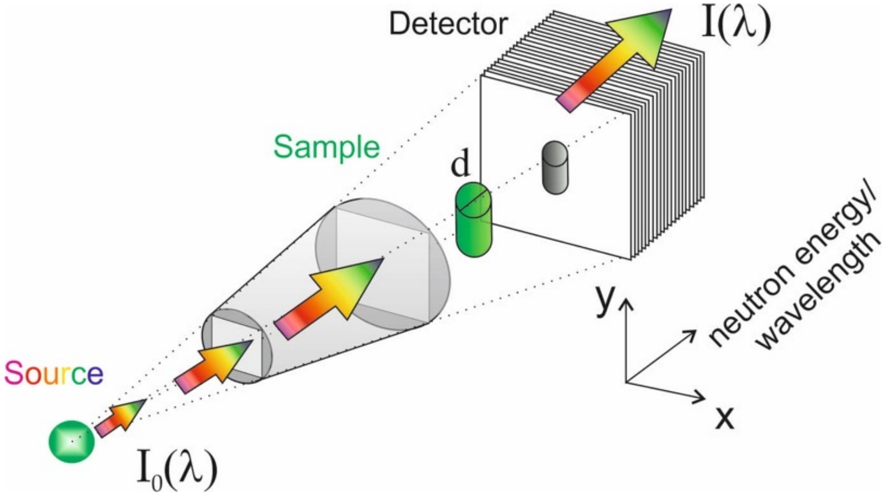

$$T(x, y, \lambda) = \frac{I(x, y, \lambda)}{I_0(x, y, \lambda)}$$

Single crystal

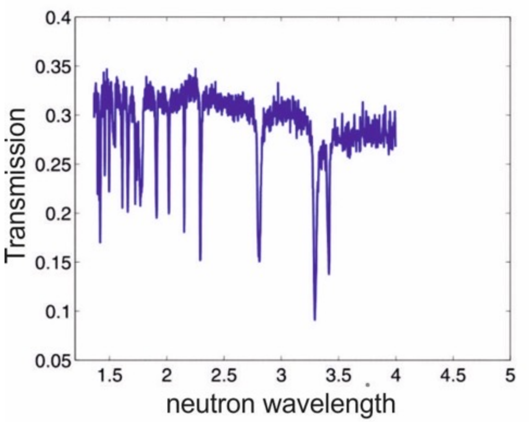

Polycrystalline materials

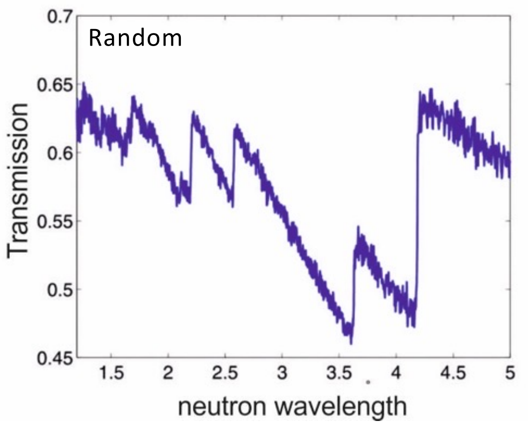

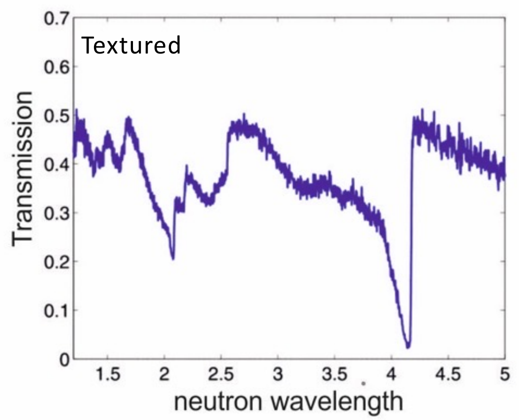

Neutron Bragg edge imaging

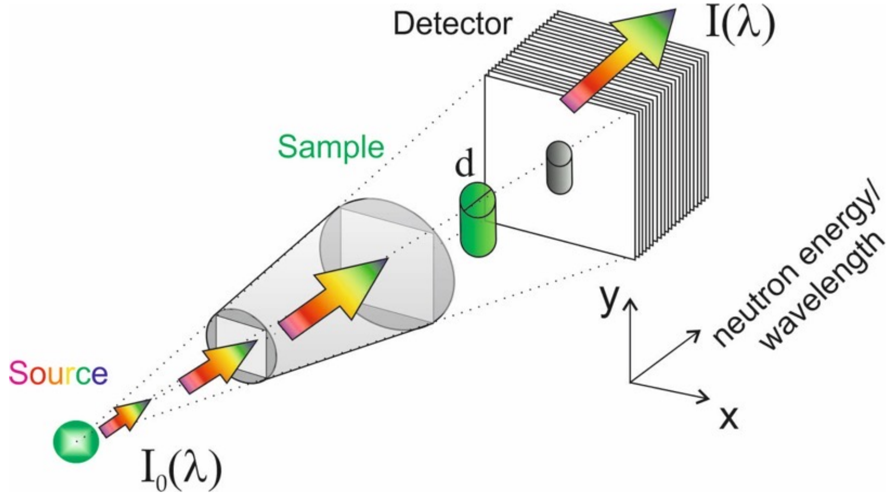

$$T(x, y, \lambda) = \frac{I(x, y, \lambda)}{I_0(x, y, \lambda)}$$

The transmission spectra contain information on the neutrons that didn't interact with the sample

⇩

All processes that remove neutrons from the incident beam

Bragg reflections

⇩

Neutrons reflected on the crystal planes

Thermal diffuse scattering

Absorption

smooth dependences on neutron wavelength

Neutron Bragg edge imaging

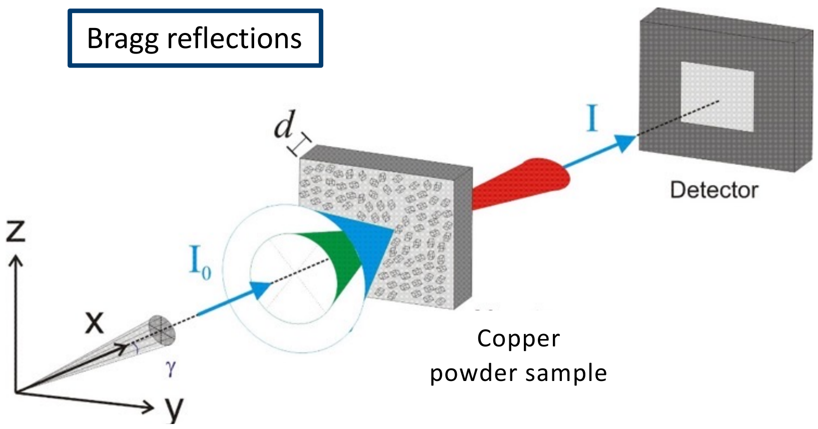

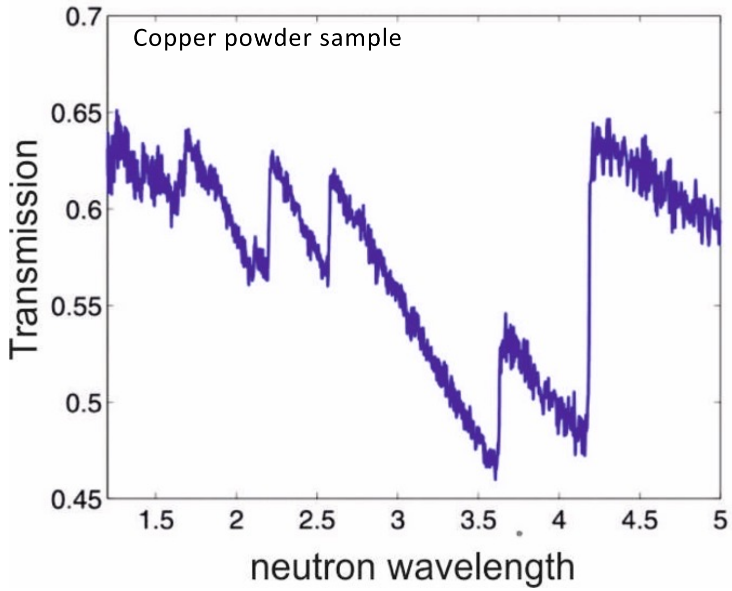

Neutron Bragg edge imaging

Bragg reflections

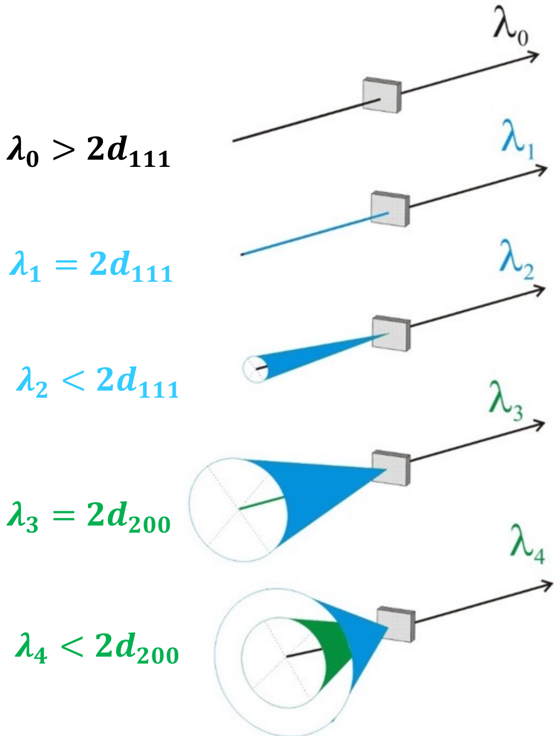

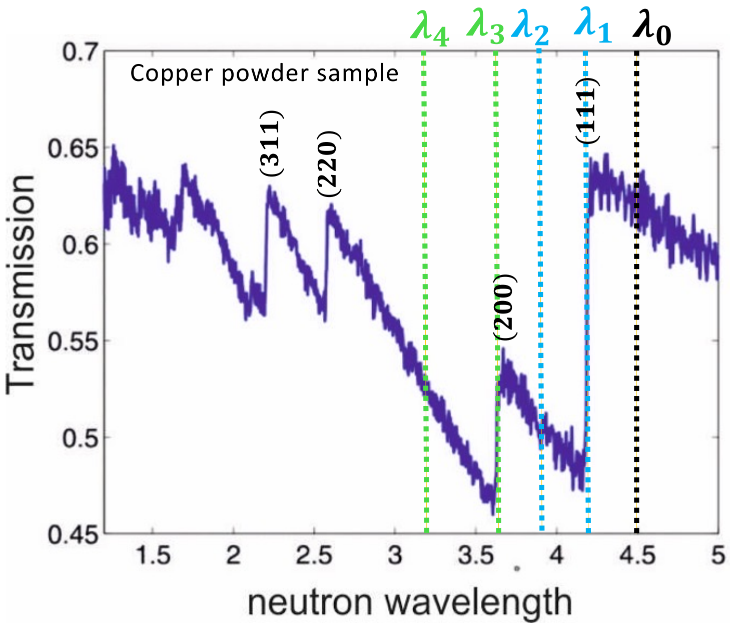

Neutron Bragg edge imaging

$$\mu(x,y,\lambda) = -\frac{1}{l}\log\left(\frac{I(x,y,\lambda)}{I_0(x,y,\lambda)}\right)$$

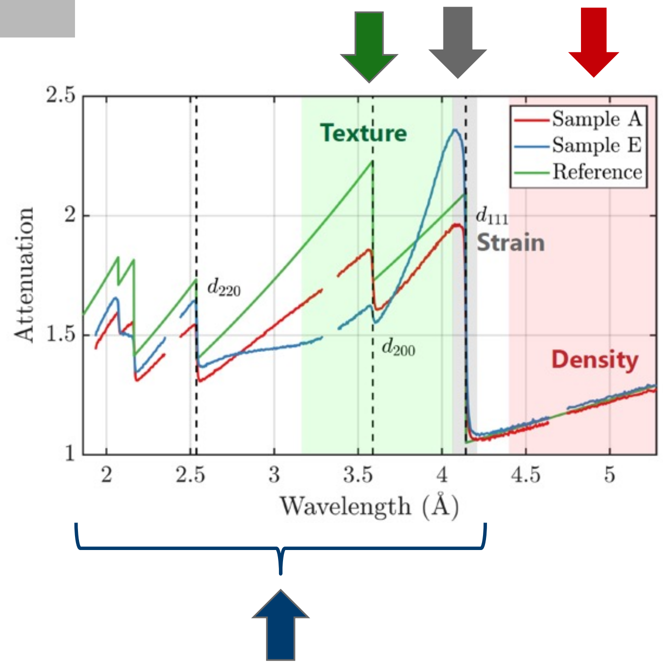

Bulk density

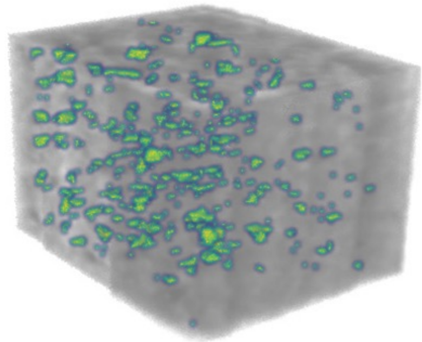

Busi, M., et al. *Ph. Rev. Mat.* (2022)

Residual Strain

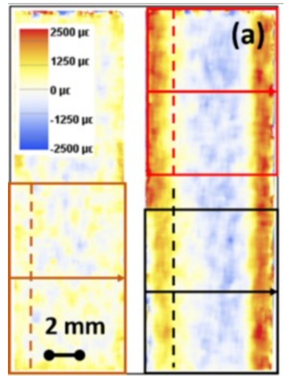

M. Morgano *et al.*, *Add. Man.* (2020)

Crystallographic Phase Transformations

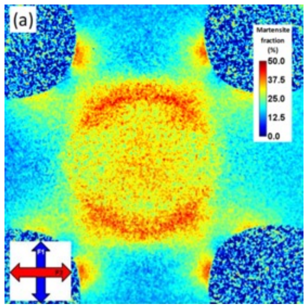

Poladitis, E., et al. *Materials* (2020)

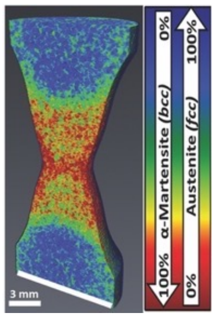

Woracek, R., et al. *Advanced Materials* (2014)

Crystallographic Texture

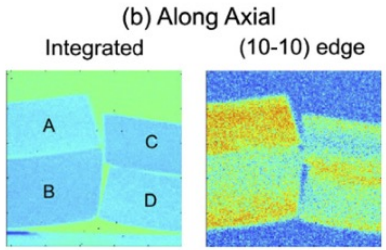

Santisteban., et al. *Journal of Nuclear Materials* (2012)

Lattice strain mapping

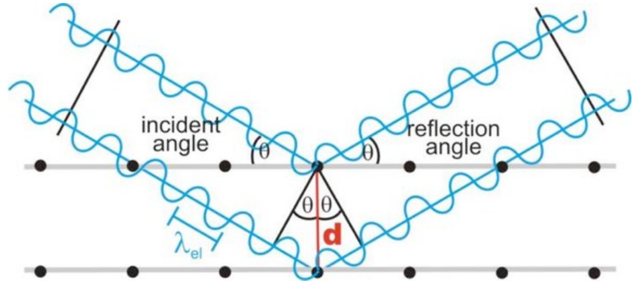

- **Bragg's law:**

$$\lambda_{hkl} = 2d_{hkl}\sin(\theta)$$

Relates Bragg edge wavelength to lattice spacing

- **Lattice strain**:

$$\epsilon_{hkl} = \frac{d_{hkl} - d^0_{hkl}}{d^0_{hkl}}$$

- **Tensile** (+)
- **Compressive** (-)

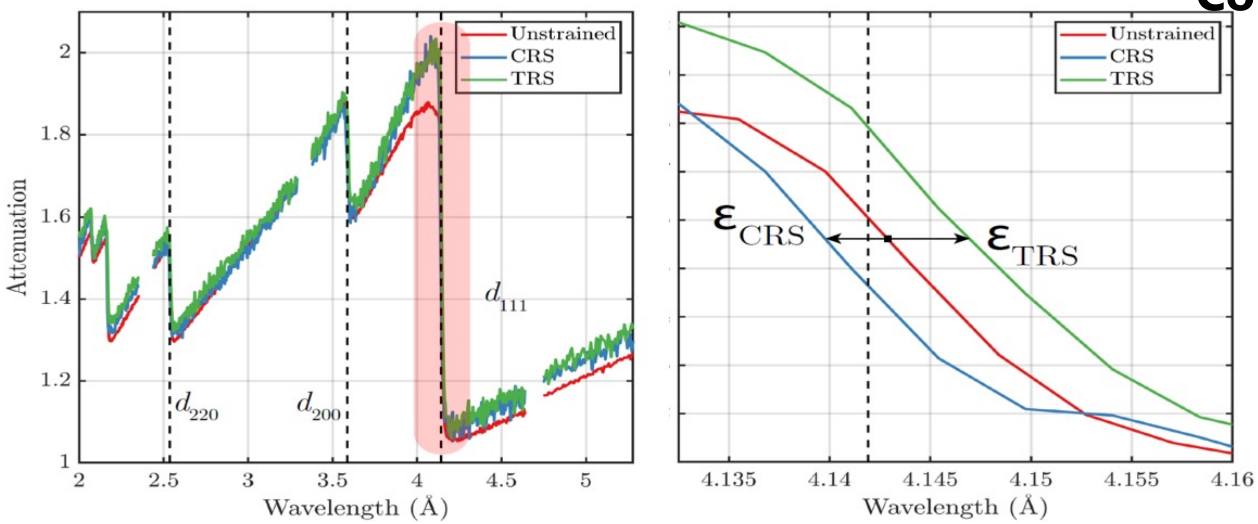

Busi, M., et al. *Scientific Reports* (2021)

Strain imaging in AM 316L

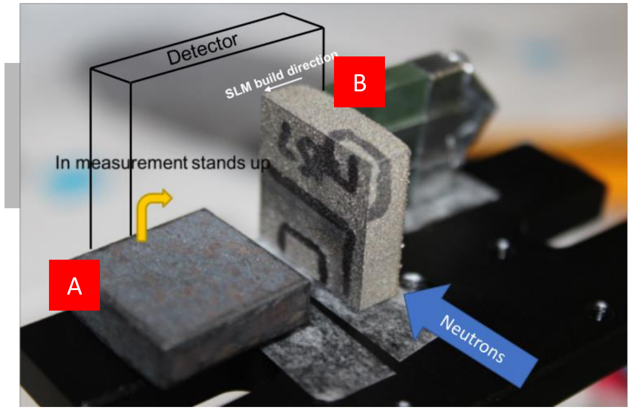

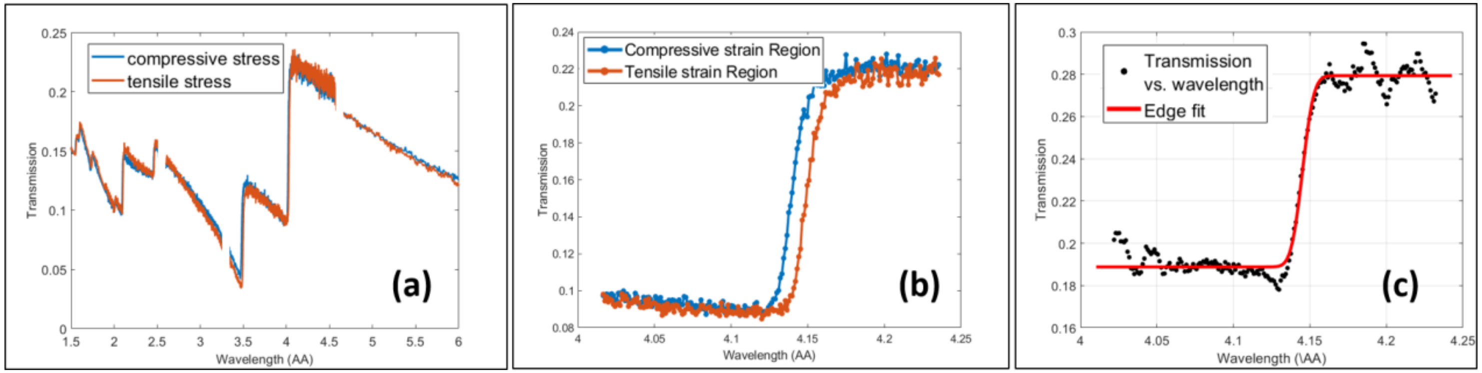

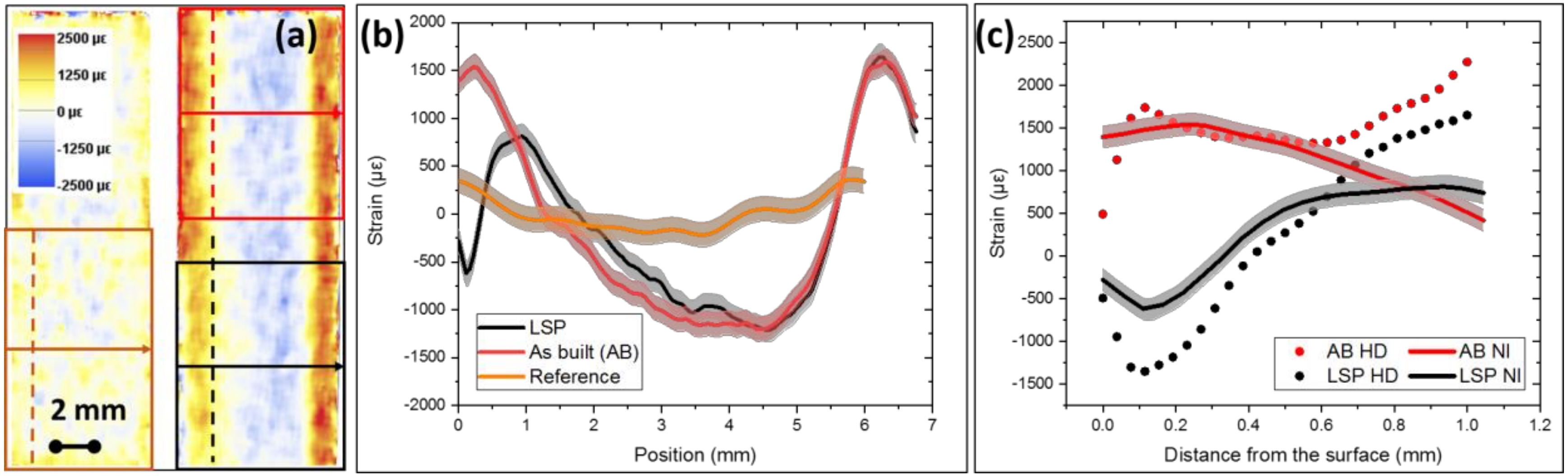

Multi-material LPBF

CuCrZr-316L layered specimens

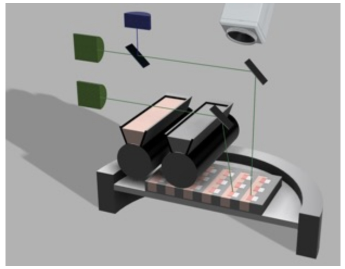

ETH zürich

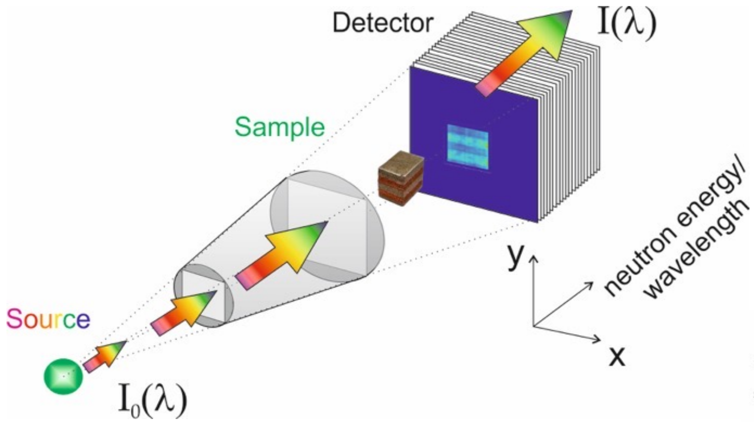

Interface

Crystallographic texture

Residual stresses

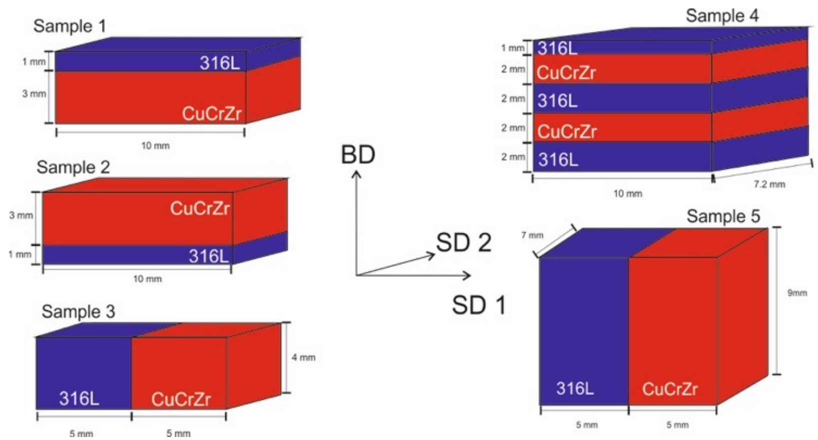

Texture characterization

Bragg Edge Imaging at BOA

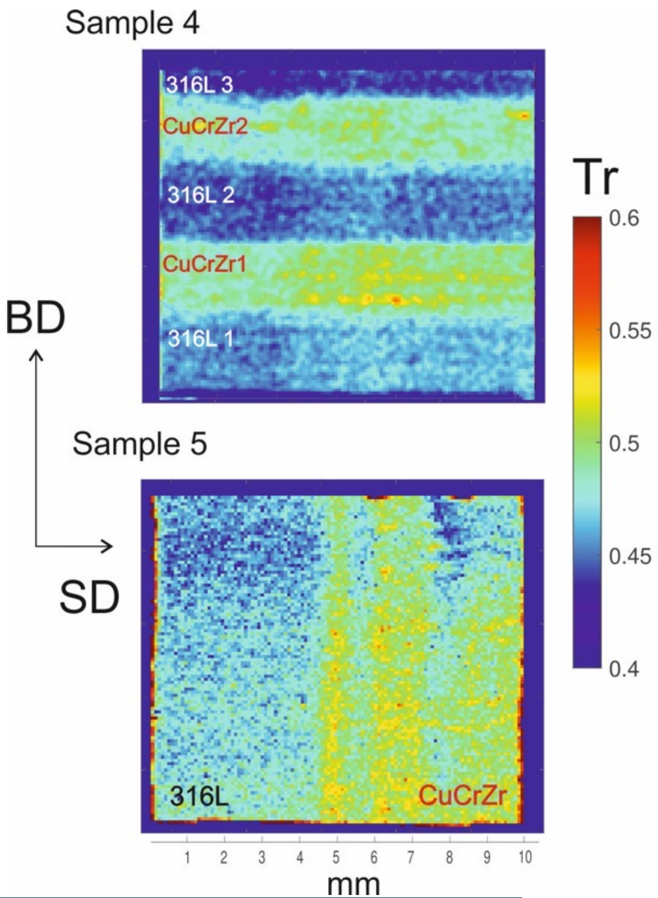

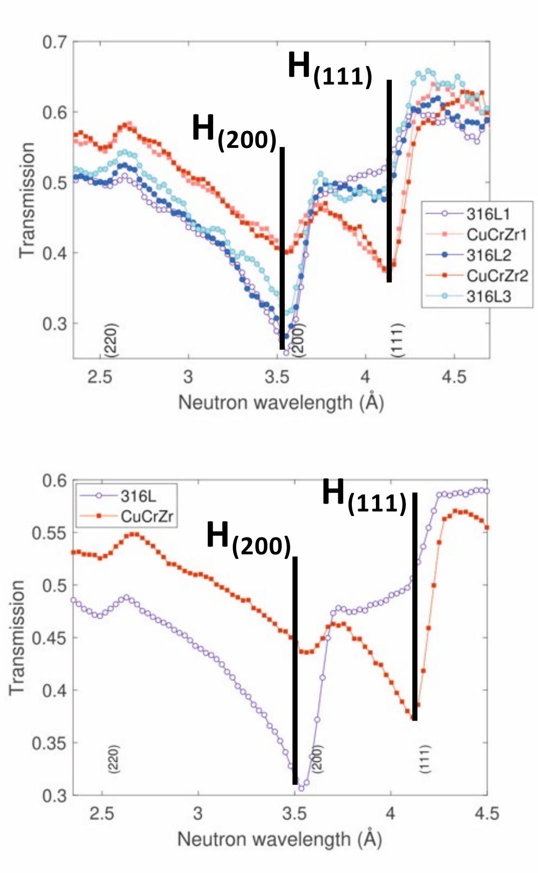

316L ⇨ Strong (200) texture along TD

Cu ⇨ Random texture along TD

Texture characterization

Bragg Edge Imaging at BOA

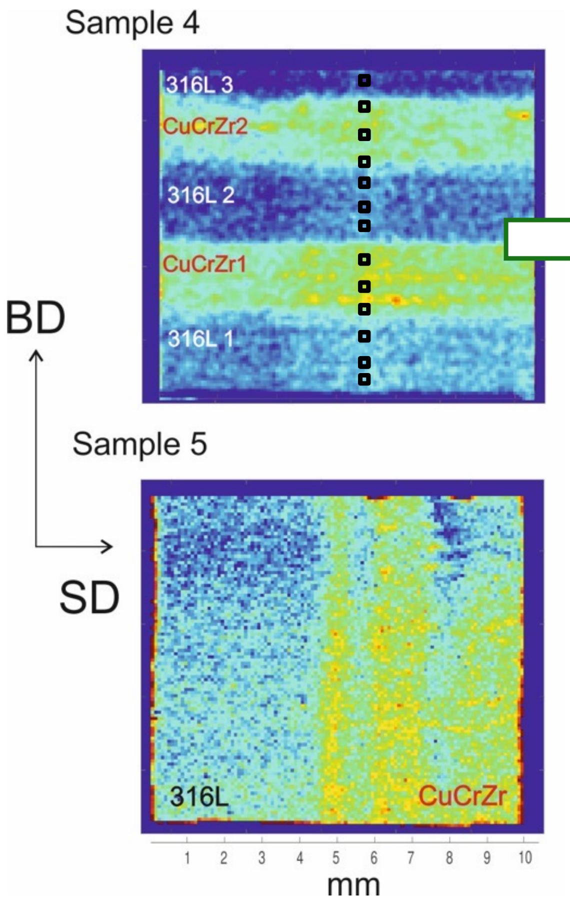

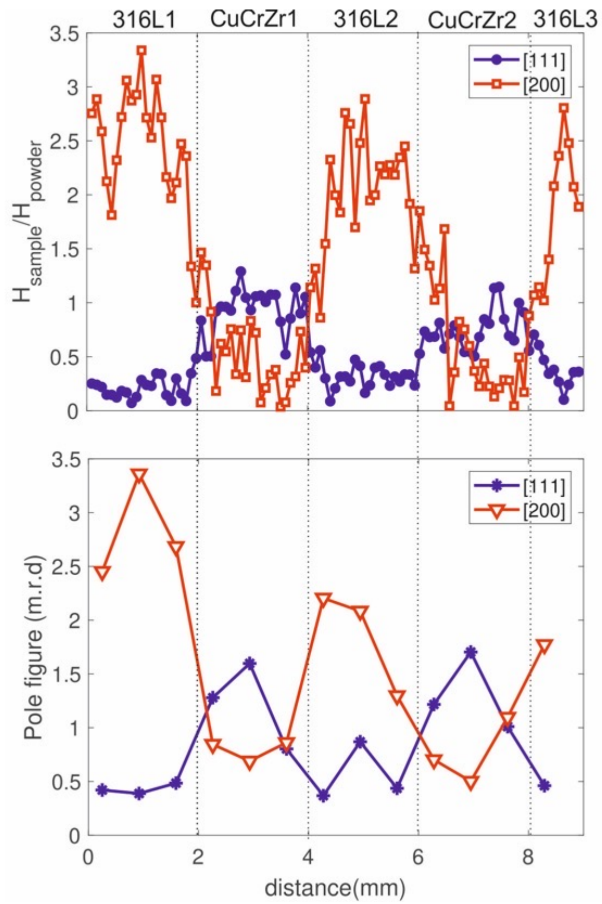

Neutron Grating Interferometry (NGI)

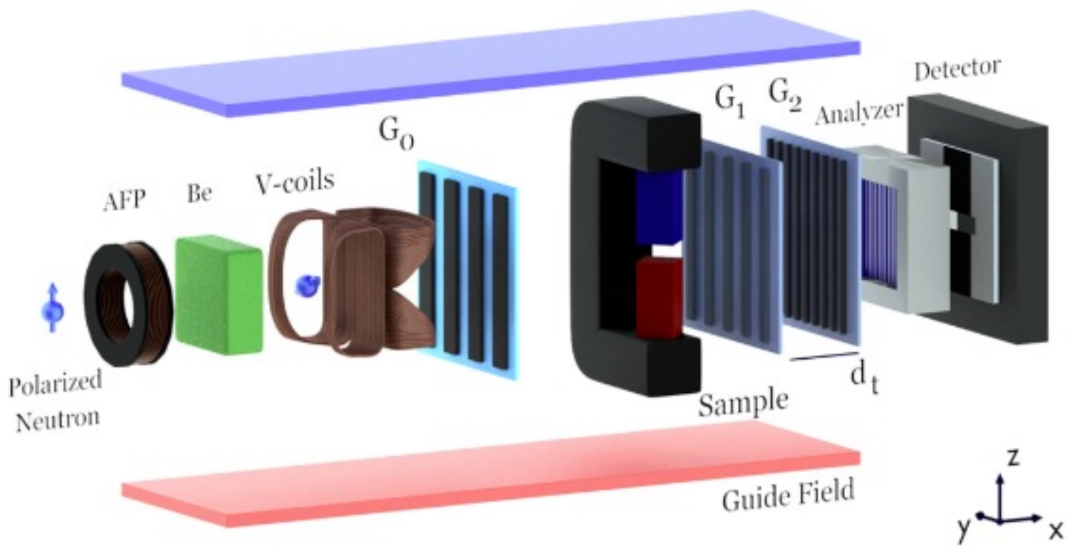

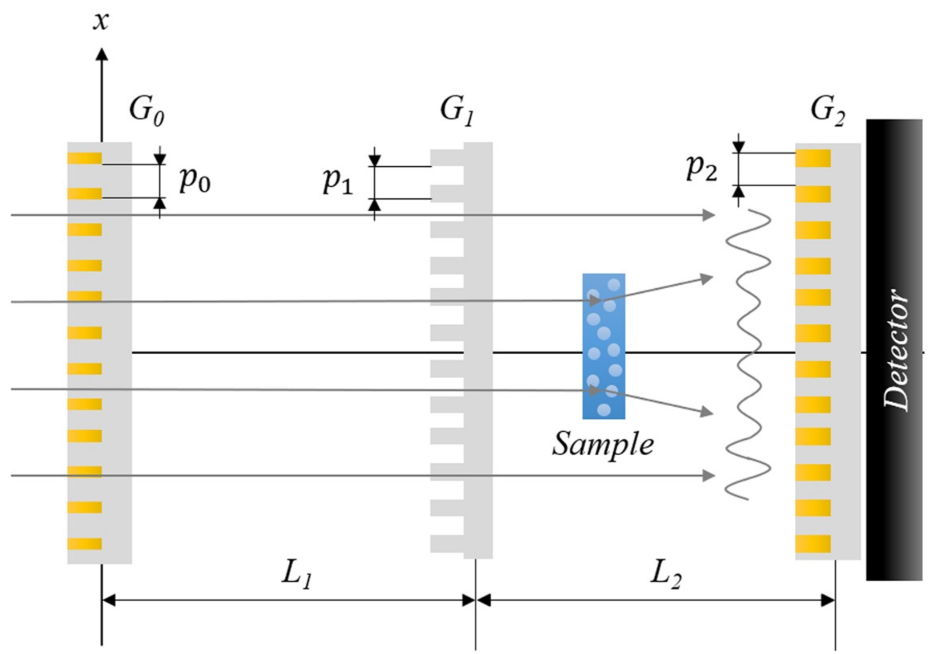

G0: source grating

G1: phase grating

G2: analyser absorption grating

Neutron Grating Interferometry (NGI)

Strobl, M., et al. *P.R.L.* (2008)

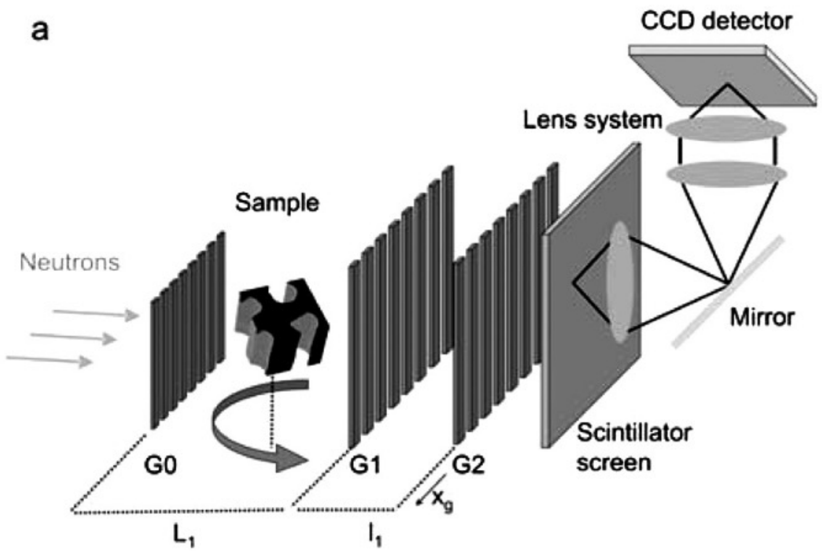

Refractive index:

$$n = \delta + i\beta$$

Measure simultaneously:

- Transmission (T) ∝ attenuation β

Transmission

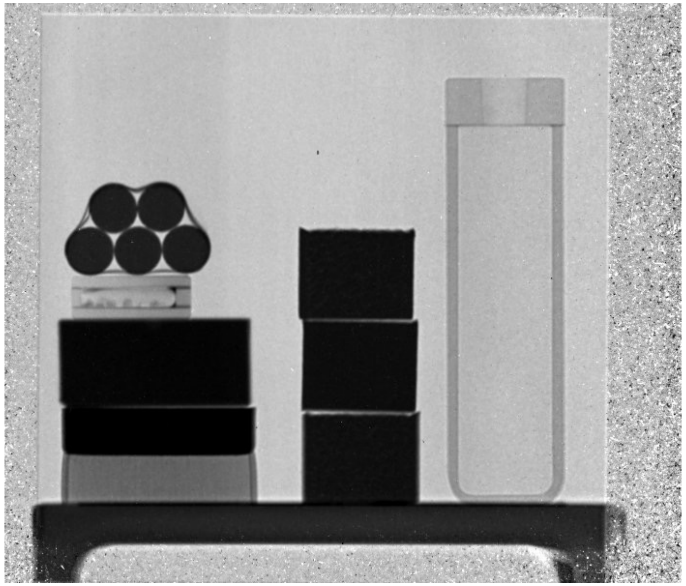

Neutron Grating Interferometry (NGI)

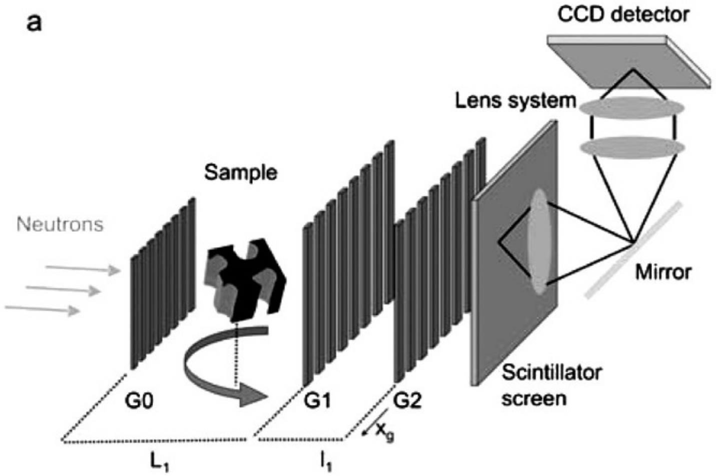

Transmission

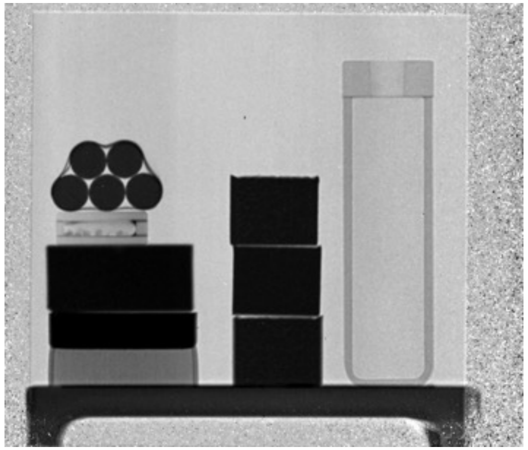

Differential phase (δ_x)

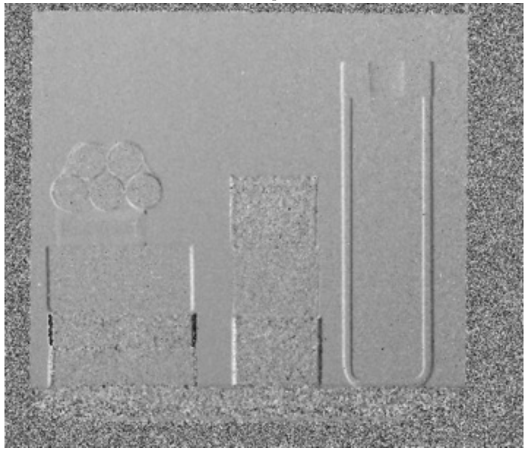

Refractive index:

$$n = \delta + i\beta$$

Measure simultaneously:

- Transmission (T) ∝ attenuation β
- Differential phase (DP) ∝ phase δ

Imaging with polarized neutrons

- **Neutron:**
  - Spin ½
  - Magnetic moment μ

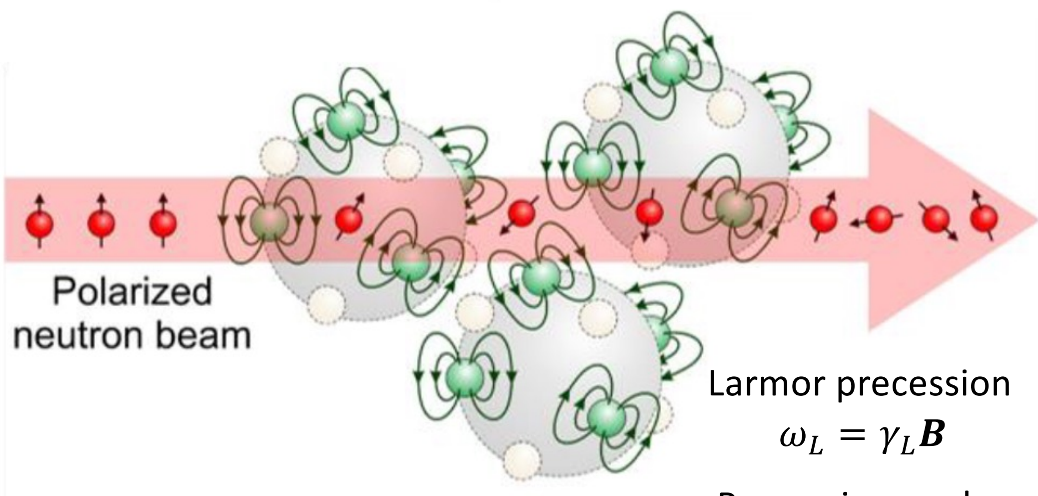

Larmor precession

$$\omega_L = \gamma_L \boldsymbol{B}$$

Precession angle:

$$\phi = \frac{\gamma_L}{v} \int_{path} B \, ds$$

Imaging with polarized neutrons

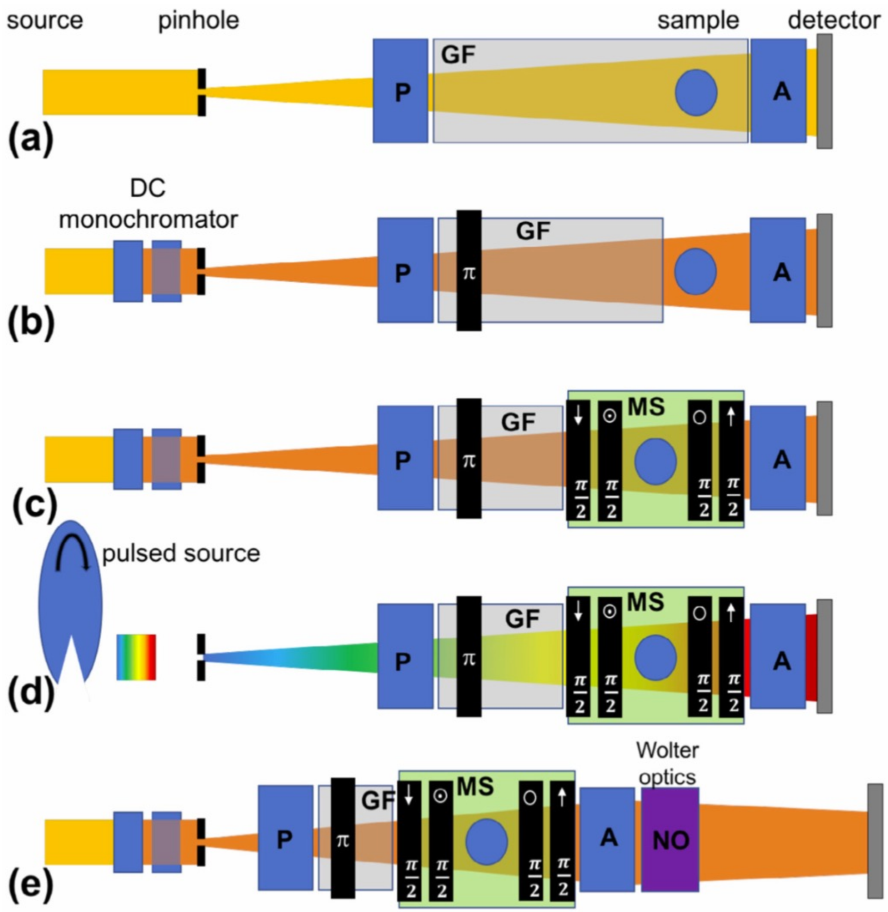

Depolarization imaging with white beam

Depolarization imaging with monochromatic beam

polarimetric neutron imaging
probing the full depolarization matrix

Imaging with polarized neutrons

- **Neutron:**
  - Spin ½
  - Magnetic moment μ

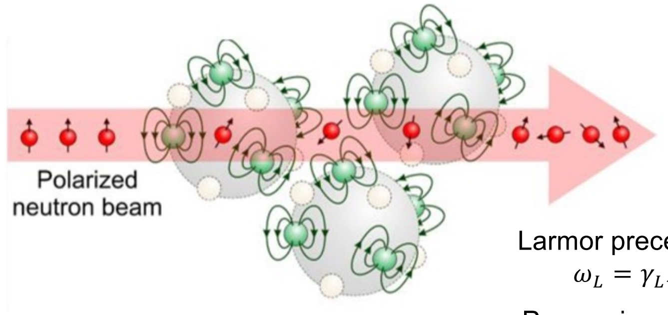

Larmor precession
$\omega_L = \gamma_L \boldsymbol{B}$

Precession angle:
$\phi = \frac{\gamma_L}{v} \int_{path} B\, ds$

- **Instrumentation:**

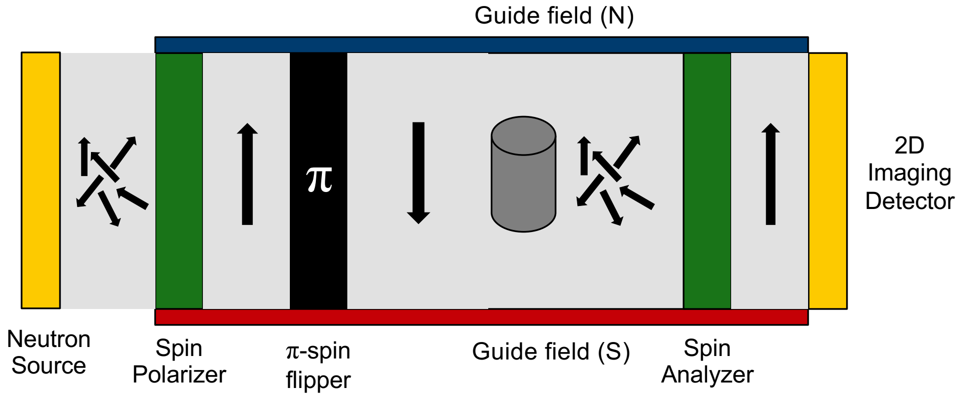

$$I = I_\uparrow + I_\downarrow$$

$$P = \frac{I_\uparrow - I_\downarrow}{I_\uparrow + I_\downarrow}$$

→

$$T = \frac{I}{I_0}$$

$$D = \frac{P}{P_0}$$

ToF-chopper and additional spin-flippers can be added

TRIP effect: martensitic phase transformation

TRIP effect: martensite transformation upon deformation

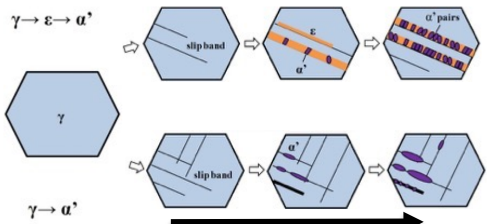

Deformation

Martensite: **ferromagnetic**

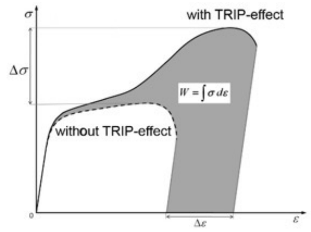

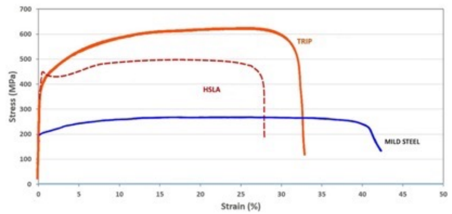

TRIP effect leads to work hardening increasing alloy's:

- **strength**
- **ductility**

Locally tailor the crystallographic **texture**, in order to **enhance** or **suppress** local transformations according to the requirements of a component.

Build complex samples with local varying material properties and thus **superior performance**

Method validation with BCC/FCC powder mixtures

$$\mu = -\frac{1}{t}\log\left(\frac{I}{I_0}\right)$$

$$\eta = -\frac{1}{t}\log\left(\frac{P}{P_0}\right)$$

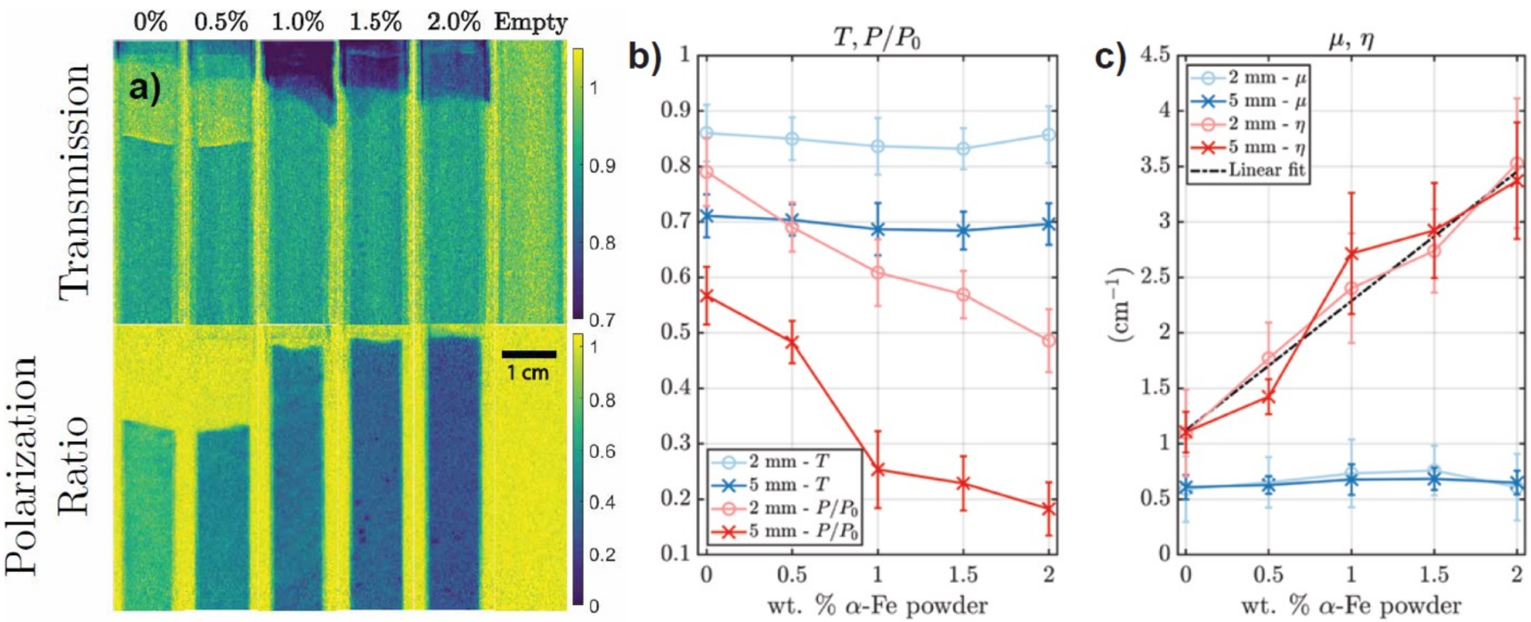

Validation of linear attenuation and depolarization coefficient for **quantitative martensite phase fraction determination**

Busi, M., et al. Materials Today Advances (2022)

In-situ tensile test

Short exposures made it possible to carry out **in-situ** measurements with a uniaxial **tensile rig**

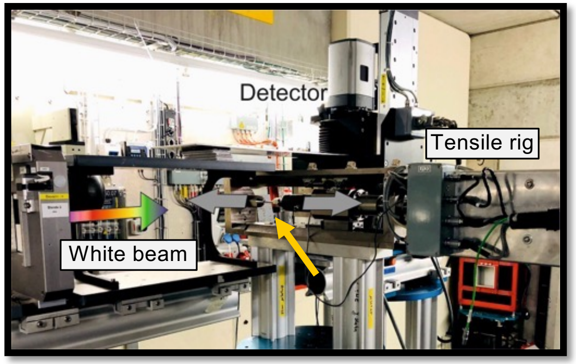

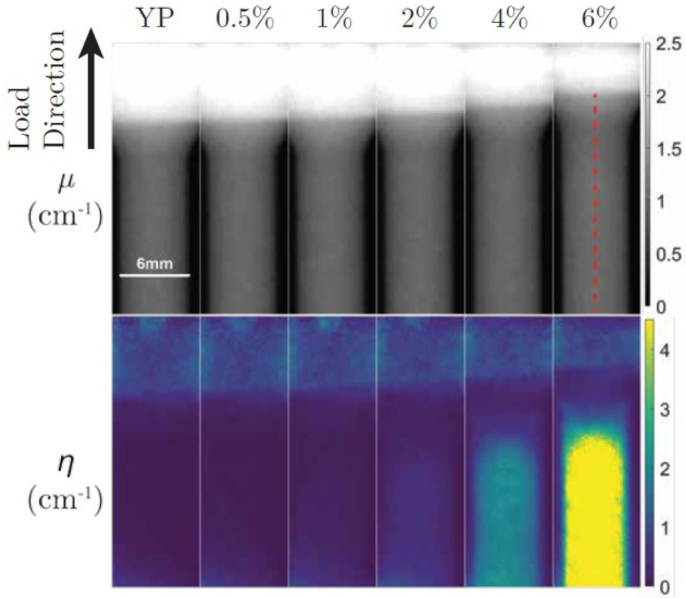

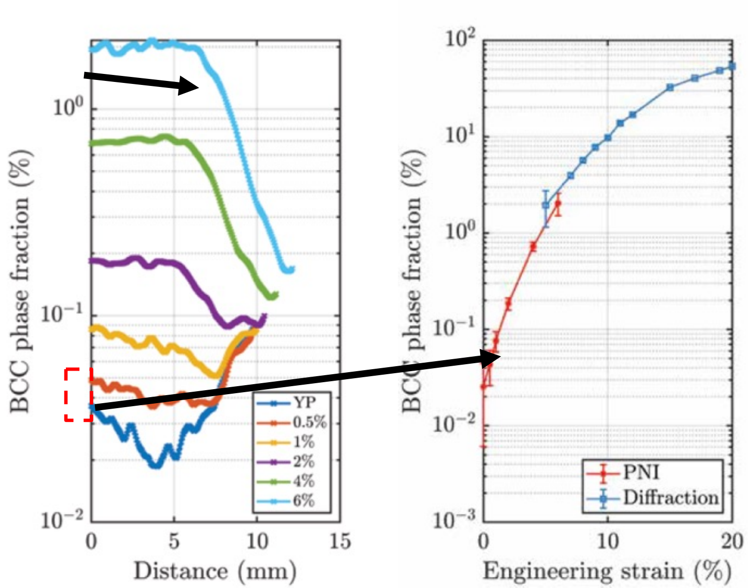

Busi, M., et al. Materials Today Advances (2022)

Shape Memory Alloys

- FeMnSi SMAs for compression energy absorption
  - Upon compression the lattice deforms
  - Heat treatment is applied for shape recovery
  - Formation of martensite is detrimental to shape recovery

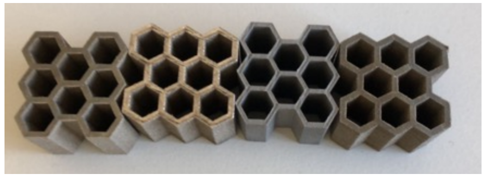

*20 seconds per frame

Time-resolved* Radiography

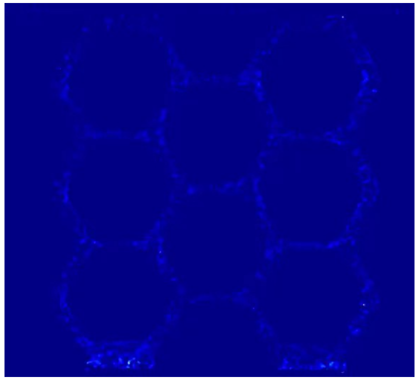

Tomography

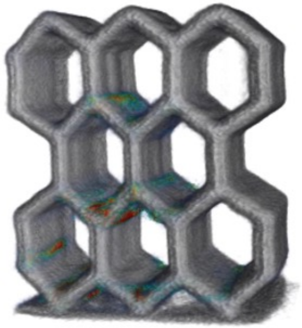

Time-resolved* Radiography

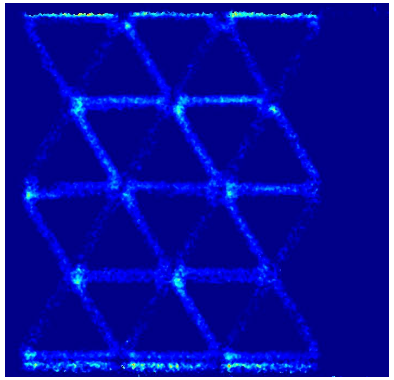

Tomography

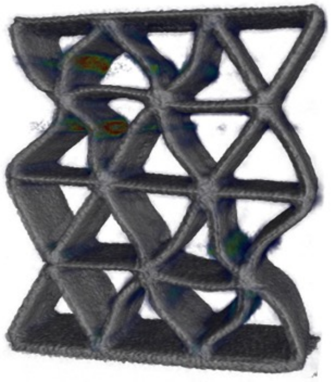

Results match well finite element analysis (FEA) simulations

Literature

- Advances in neutron imaging, Materials Today 21, 6252 (2018)
- Detailed talk on neutron tomography: https://www.youtube.com/watch?v=s95mKjlKm_c
- Introduction talk: https://www.youtube.com/watch?v=tyWTzrnRH9U